Investigation of subsurface hydrology of a Chalk Cliff in Normandy Using Multiple Research Approaches

Thomas Junique[1,2], Ao Wang[1], Georges Sadaka[1,3], **Raphaël Antoine**[2], Cyrille Fauchard[2], Antoine Tonnoir[4], Stéphane Costa[5], Olivier Maquaire[5], Faycal Réjiba[6], Robert Davidson[5], Nicolas Coppo[7]

[1] Cerema, ENDSUM
[2] Université de Reims Champagne-Ardenne
[3] Université de Rouen-Normandie, LMRS
[4] LMI, INSA Rouen
[5] Université de Rouen-Normandie, UMR IDEES
[6] Université de Caen-Normandie, M2C
[7] BRGM

Characterization and understanding of the processes causing the retreat of cliff coasts

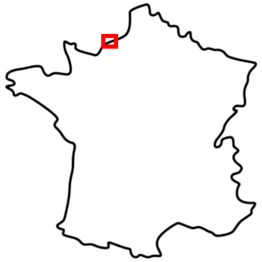

Sudden collapse

↓

High rates of coastal erosion

0,09 $m.a^{-1}$ to 0,23 $m.a^{-1}$ from the top of the cliff between Cap d'Antifer and Tréport*.	Cap d'Ailly * : 0,80 $m.a^{-1}$

↓

Erosion factors

Lithology, fracture pattern (physical degradation by freeze-thaw), degree of water saturation, subaerial and marine water movement (wetting/drying, chemical weathering, or salt crystallization, etc.)

Seawater intrusion ?

*Duperret et al., 2005; Lissak et al., 2013; Maquaire et al., 2019

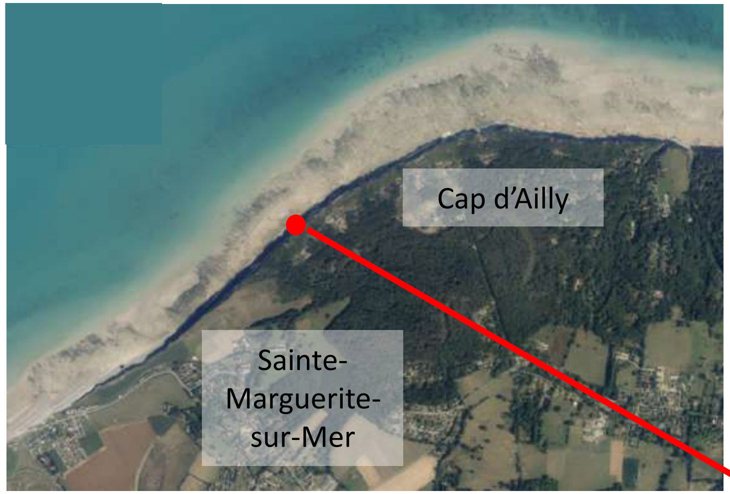

DEFHY3GEO Region Project : Detection and Study of Fracturing by HYdrological, GEOmorphodynamic, GEOlogical and GEOphysical approach

Monitoring/studying cliffs with various approaches and techniques

Data processing

Electrical, Ground Penetrating Radar, seismic, TDEM and EMI methods

Instrumental station

Piezometer

Drone Visible Infrared

Coastal cliff

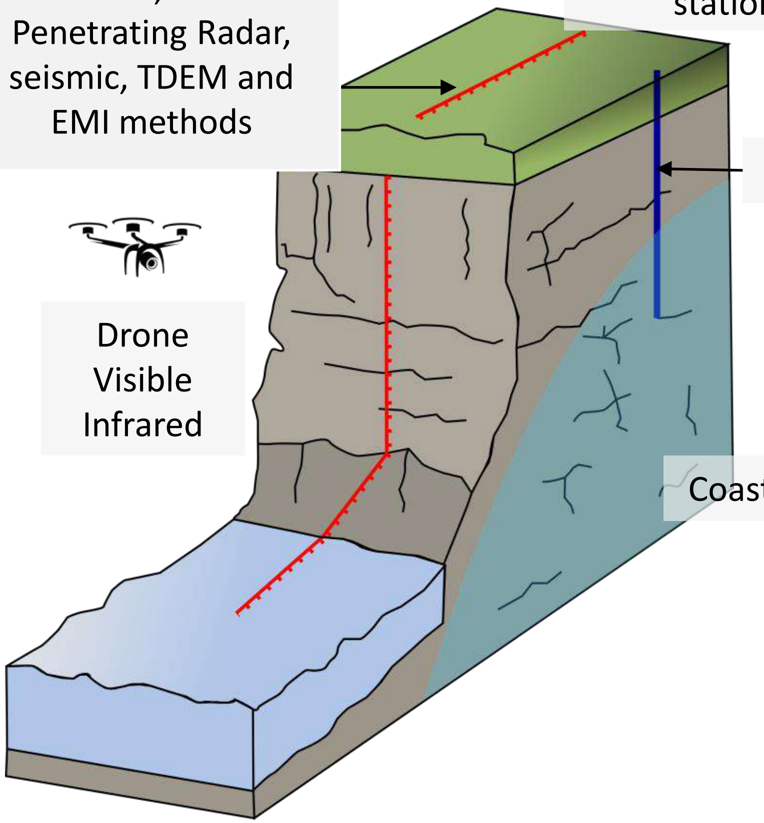

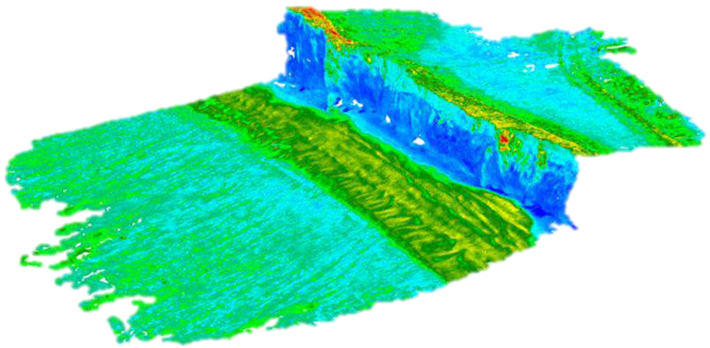

3D models (digital elevation models or DEM)

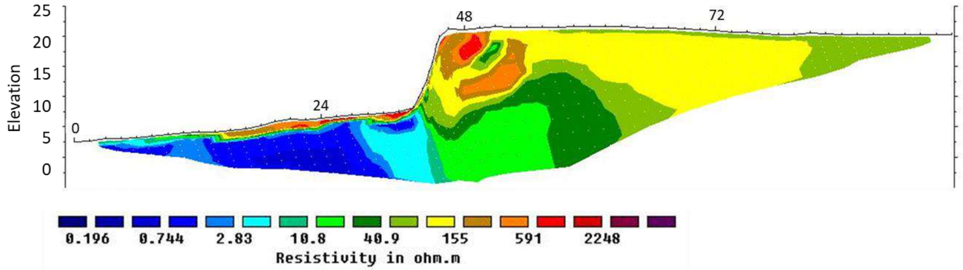

Electrical resistivity tomography (ERT)

Structural model (geometry, stratigraphy)

Hydrogeological model

How saline water interact with freshwater within the cliffs ?

Location of geophysical measurements

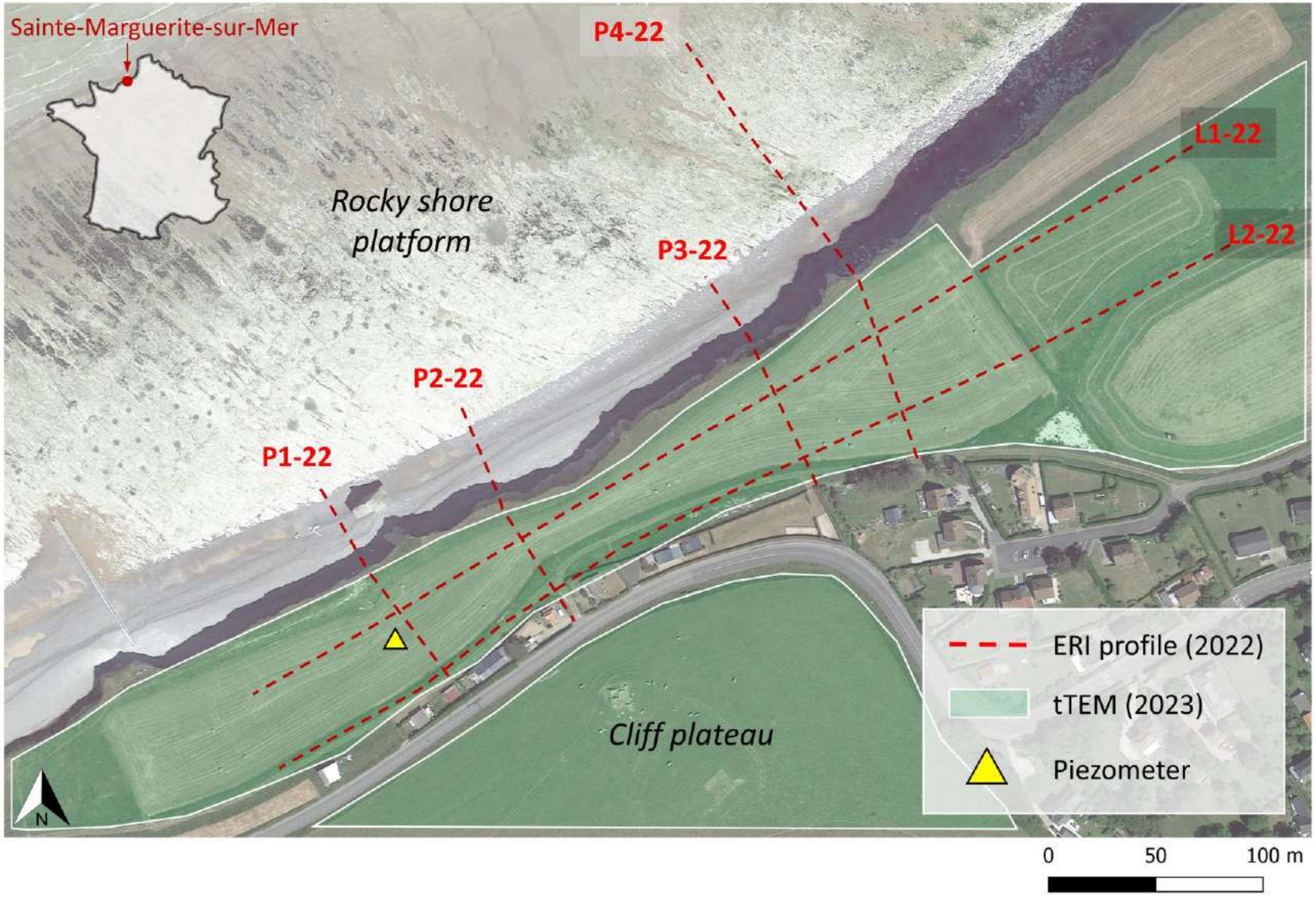

- Aerial measurements by drone (visible and TIR wavelengths)
- 6 Electrical resistivity tomography (ERT)
- Towed Time Electromagnetic Method (tTEM)
- Piezometer


Steeplejacks for ERT on cliffs


DGNSS of all electrodes


tTEM with quad


Drone with TIR and visible camera

How to obtain a reliable electrical image inside of the cliff ?
The influence of complex topography on inversions

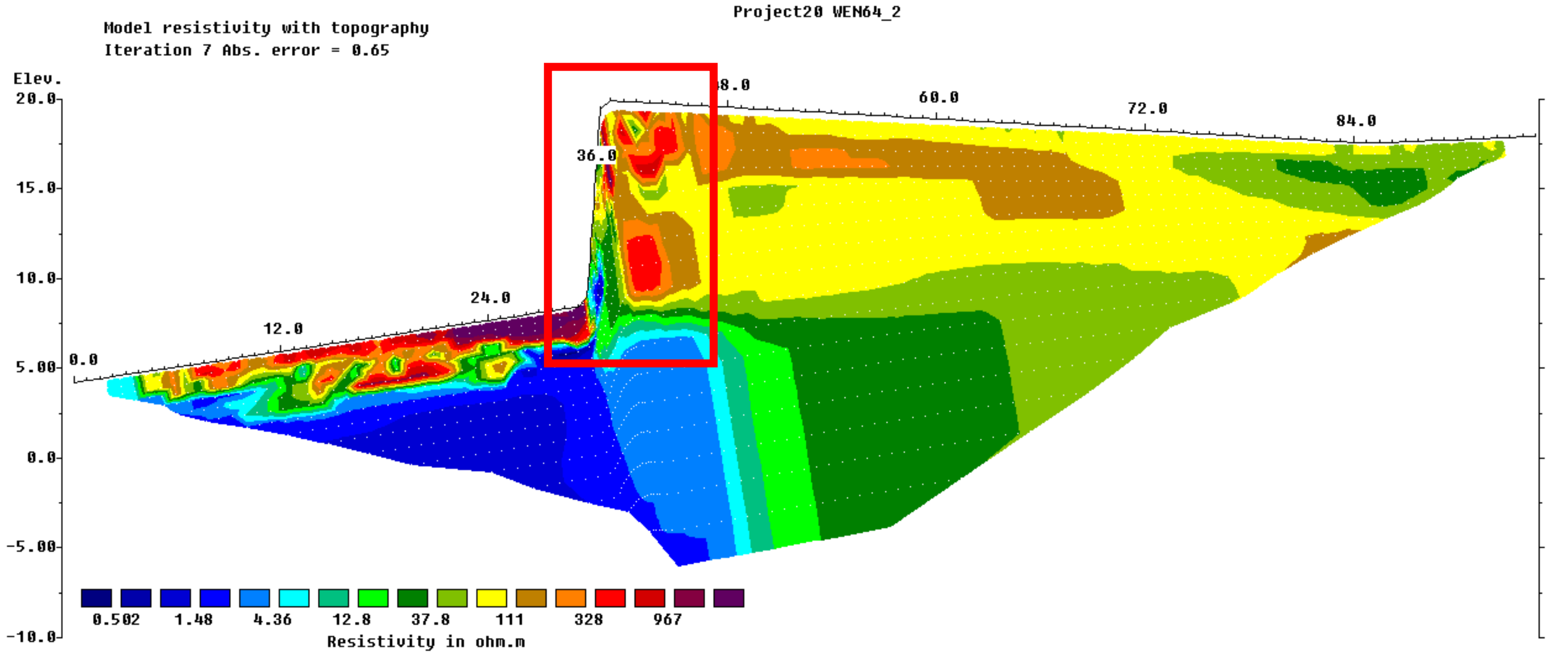

Huge deformations of the grid and artefact generation
at the cliff wall

How to obtain a reliable electrical image inside of the cliff ?
The influence of complex topography on inversions

A first classical ERT survey in 2017

- Need to better constraint inversion
- And take into account for complex DEMs

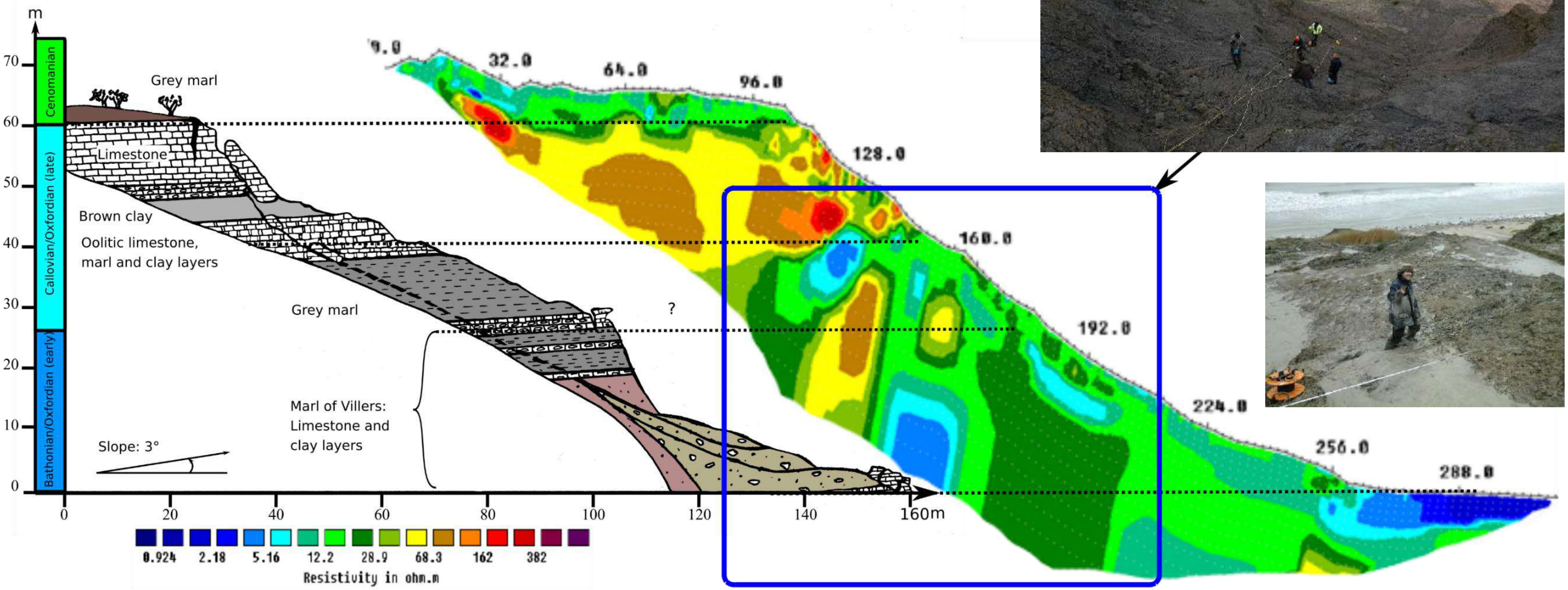

How to obtain a reliable electrical image inside of the cliff ?
The influence of complex topography on inversions

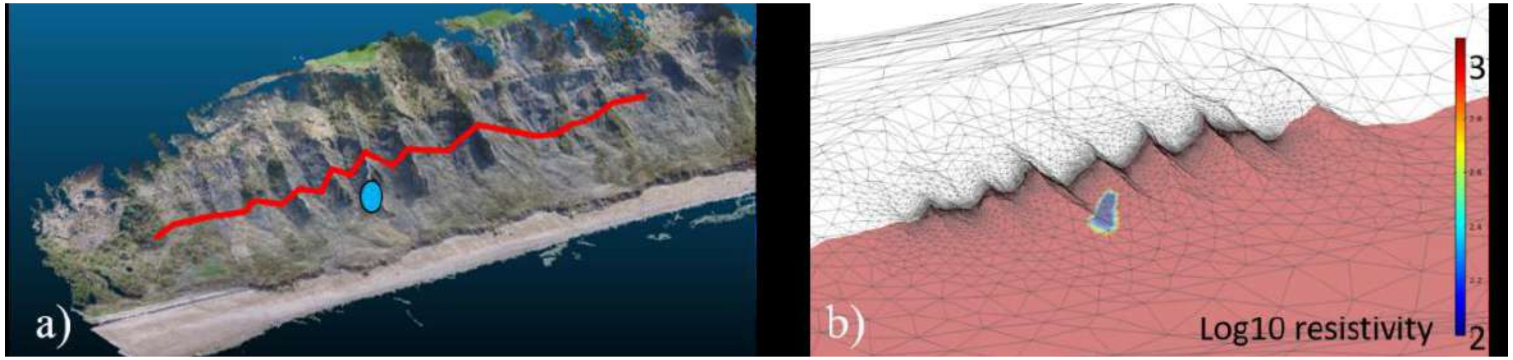

a) Point cloud of the case study. Red line shows the location of the ERT Profile. A blue sphere symbolizes the synthetic anomaly. b) 3D FEM of the case study with a local synthetic anomaly located beneath the ERT profile (Fargier et al., 2021).

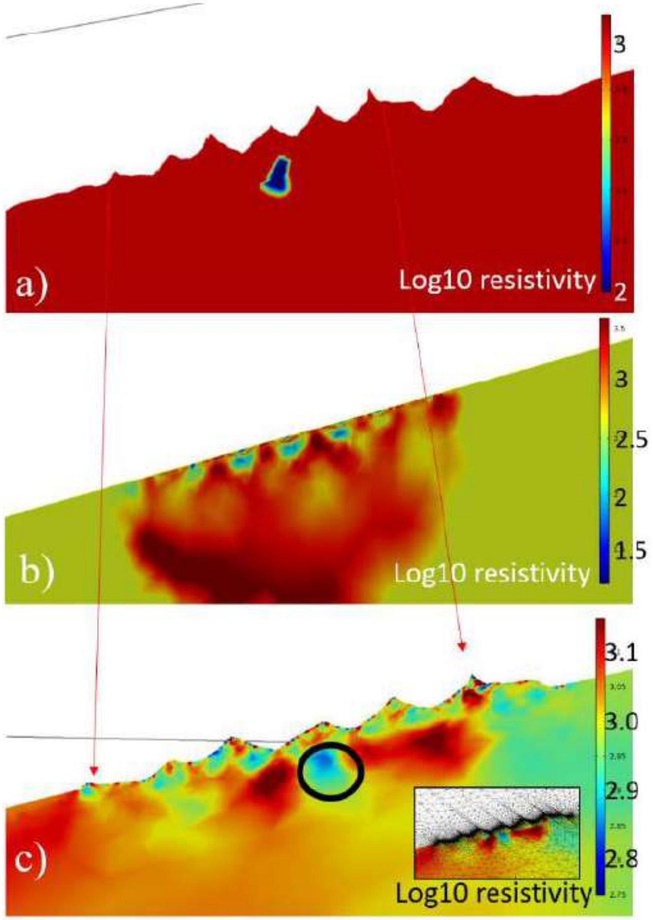

2D slices extracted from a 3D resistivity distribution. a) "True model". b) inversion result without topography information. c) inversion result with a 2D assumption of the topography.

The problem of topography : the birth of the open source PyLGRIM*ff* software

Python-based Language for Geoelectrical Resistivity Imaging and Modelling using Frem Fem

The need

- Accurate description of ground topography, especially around electrodes
- Take into account non-aligned electrodes -> full 3D forward problem
- Consistent boundary conditions
- Reasonable memory cost.

The solution

- Procedure based on the use of GMSH to integrate any digital elevation model
- Handle several electrodes profiles to generate a mesh taking into account 3D position of the profiles
- New aspect to take into account unbounded domain using infinite element together with conventionnal finite elements.

Tonnoir et al., 2024 (Computers and Geosciences)

Python-based Language for Geoelectrical Resistivity Imagery Modelling using FreeFem

Mathematical formulation of the direct problem :
Find the potentiel V satisfying the following PDE system

$$\begin{cases} -\vec{\nabla} \cdot \left(\sigma \vec{\nabla} V \right) = c_{\mathcal{E}} \delta_{x_{\mathcal{E}}, y_{\mathcal{E}}, z_{\mathcal{E}}} & \text{in} \quad \mathcal{V} \\ \sigma \vec{\nabla} V \cdot \vec{n} = 0 & \text{on} \quad \mathcal{S} \cdot \\ \lim_{\infty} V = 0 & \end{cases} \tag{5}$$

where $\delta_{x_{\mathcal{E}}, y_{\mathcal{E}}, z_{\mathcal{E}}}$ is the Dirac distribution located at the electrode position $(x_{\mathcal{E}}, y_{\mathcal{E}}, z_{\mathcal{E}})$ and $c_{\mathcal{E}}$ is a constant that represents the current density injected on the electrode $\mathcal{E}$. It is known that this problem has a unique solution V (Hadamard, 1902).

Python-based Language for Geoelectrical Resistivity Imagery Modelling using FreeFem

Discretization aspect

Variational formulation of the problem consist to find V solution for any test function Psy.

$$a(V,\Psi) = c_{\mathcal{E}}\Psi(x_{\mathcal{E}}, y_{\mathcal{E}}, z_{\mathcal{E}}), \quad \text{where} \quad a(V,\Psi) = \int_{\mathcal{V}} \sigma \nabla V \cdot \nabla \Psi \, d\mathcal{V}. \qquad (8)$$

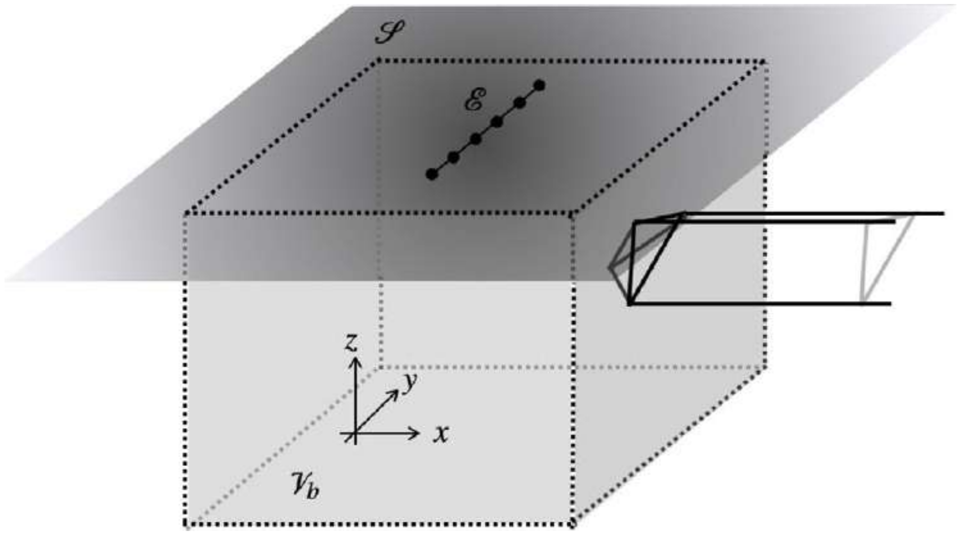

Fig. 3. Representation of the support of an infinite element test function lying on the boundary $\{x = x_{max} + L_x\}$. In the interior domain $\mathcal{V}_b$, the tetrahedron is represented.

To numerically solve this problem, a finite element space is considered to discretize the unknown V.

Bounded domain based on a classical mesh : usual Langrange finite element discretization

Unbounded domain : the test functions are defined as the tensor product of classical Lagrange finite elements on triangle, representing the faces of the tetrahedron on artificial boundaries and a decay function with infinite support.

Python-based Language for Geoelectrical Resistivity Imagery Modelling using FreeFem

Discretization aspect

More precisely, we consider Ψ a Lagrange test function in $\mathcal{V}_b$ such that Ψ is not null on the boundary $\{x = x_{max} + L_x\}$ for instance, and let

$P(y,z) = \Psi(x_{max} + L_x, y, z)$. Then, we define the associated function as follows:

$$N(x,y,z) = P(y,z)D(|x - x_{max} - L_x|), \quad \text{with} \quad \begin{cases} D(0) = 1 \\ D(x) \underset{x\to+\infty}{\longrightarrow} 0 \end{cases} \cdot \qquad (9)$$

Note that we impose $D(0) = 1$ to ensure the continuity of the test function. Similarly, we can defined the infinite elements on the boundaries $\{x = x_{min} - L_x\}$, $\{y = y_{min} - L_y\}$, $\{y = y_{max} + L_y\}$ and $\{z = z_{min} - L_z\}$ of $\mathcal{V}_b$.

Carefull attention must be brought to the elements on the edge and on the corners of the artificial boundary

Python-based Language for Geoelectrical Resistivity Imagery Modelling using FreeFem

Inverse problem

The discretization of the direct problem (8) with infinite elements leads to solve a linear system of the form:

$$\mathbb{K}(\vec{\sigma})\vec{V} = \vec{F},$$

where $\vec{V} \in \mathbb{R}^n$ represents the potential solution on each nodes of the mesh, $\vec{F}$ the source term and $\vec{\sigma} \in \mathbb{R}^p$ the conductivity in each cell of the mesh, supposed to be constant (p being the number of cells).

Python-based Language for Geoelectrical Resistivity Imagery Modelling using FreeFem

Inverse problem

Then, the data $\vec{d}_{exp}$ can be expressed as follows:

$$\begin{aligned} \vec{d}_{exp} &= \mathbb{O}\vec{V} + \vec{\eta}, \\ &= \mathbb{O}\left[\mathbb{K}(\vec{\sigma}_{ex})\right]^{-1}\vec{F} + \vec{\eta}, \end{aligned} \tag{14}$$

where $\vec{\eta}$ represents the noise and $\vec{\sigma}_{ex}$ is the exact parameter we are looking for. Classically, the idea is to formulate the inverse problem as a minimization problem: Find the conductivity $\vec{\sigma}$, that minimizes

$$J(\sigma) = \frac{1}{2}\|\vec{d}_{exp} - \mathbb{O}\left[\mathbb{K}(\vec{\sigma})\right]^{-1}\vec{F}\|_2^2 + \frac{\varepsilon}{2}\mathcal{R}(\vec{\sigma}), \tag{15}$$

where the first term above corresponds to the discrepancy to the data, and the second term $\mathcal{R}(\vec{\sigma})$ to the regularization term (which accounts for our a priori knowledge on the medium). The parameter $\varepsilon > 0$ corresponds to the weight given to the regularization part. In our case,

Purpose : to reconstruct the conductivity $\vec{\sigma}$ in each cell given apparent resistivity measurements on the surface, that we will denote by a vector $\vec{d}_{exp} \in \mathbb{R}^m$, where m is the number of data.

Observation operator O is represented by an $m \times n$ matrix that maps the solution $\vec{V}$ of the (discretized) direct problem to the observations.

Digital Elevation Model (DEM) and 3D-inverted ERT profiles

Global view with DEM (Metashape) and ERT profiles inverted with PyIGRIMff (and ResIPy)

- All electrodes DGNSS located
- Schlumberger protocoles
- 3 days on the field

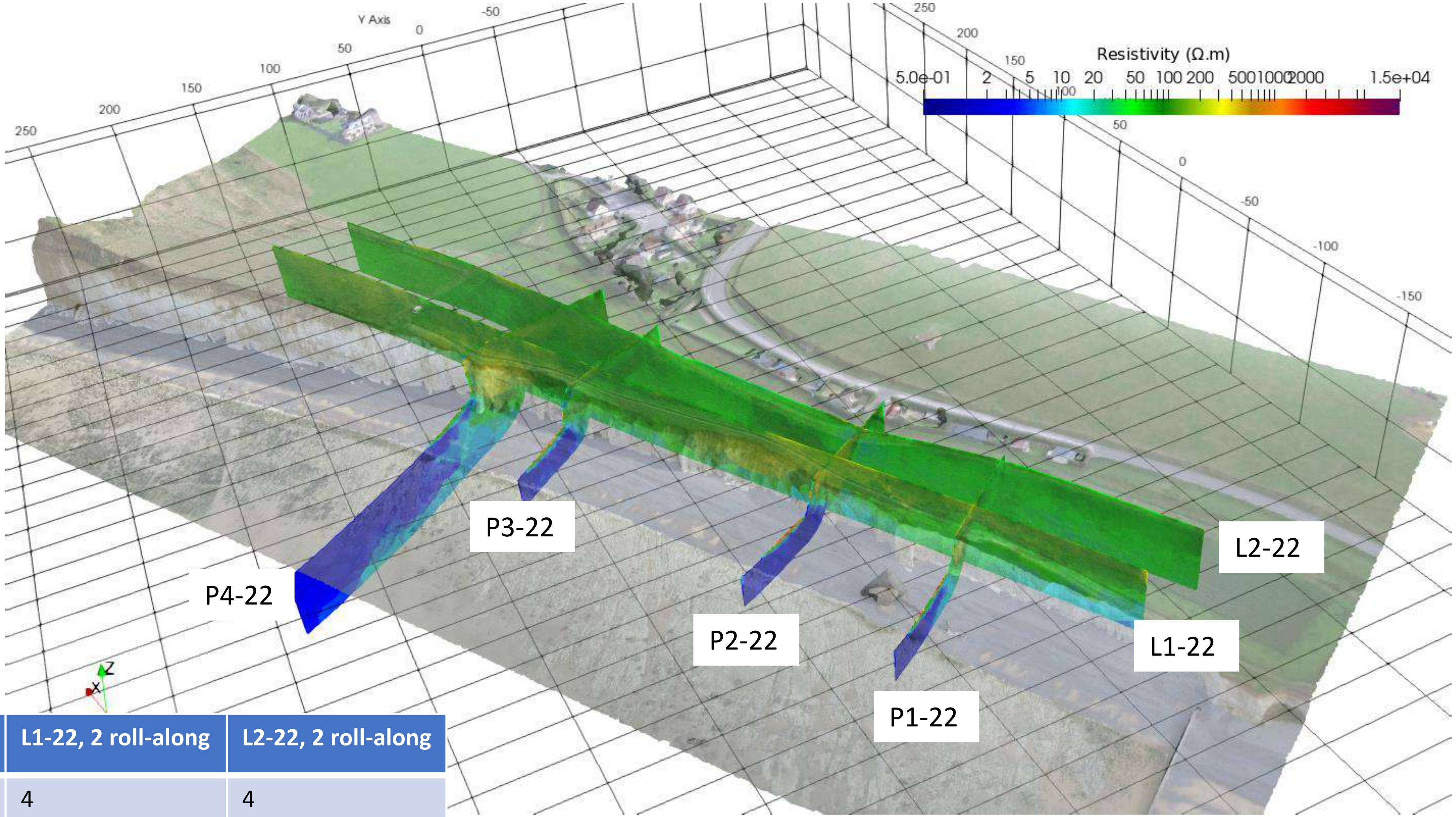

ERT name	P1-22	P2-22	P3-23	P4-24	L1-22, 2 roll-along	L2-22, 2 roll-along
Spacing	2	2	2	2	4	4
Nb quad.	989	1034	4042	2977	2532	2525
Length (m)	126	126	126	248	508	508

Digital Elevation Model and 3D-inverted ERT profiles : Interpretation

Chalk resistivity:
- very heterogeneous at the top
- Lower in depth from the plateau

Uprising brackish water

Water intrusion under the cliffs

Saturated chalk

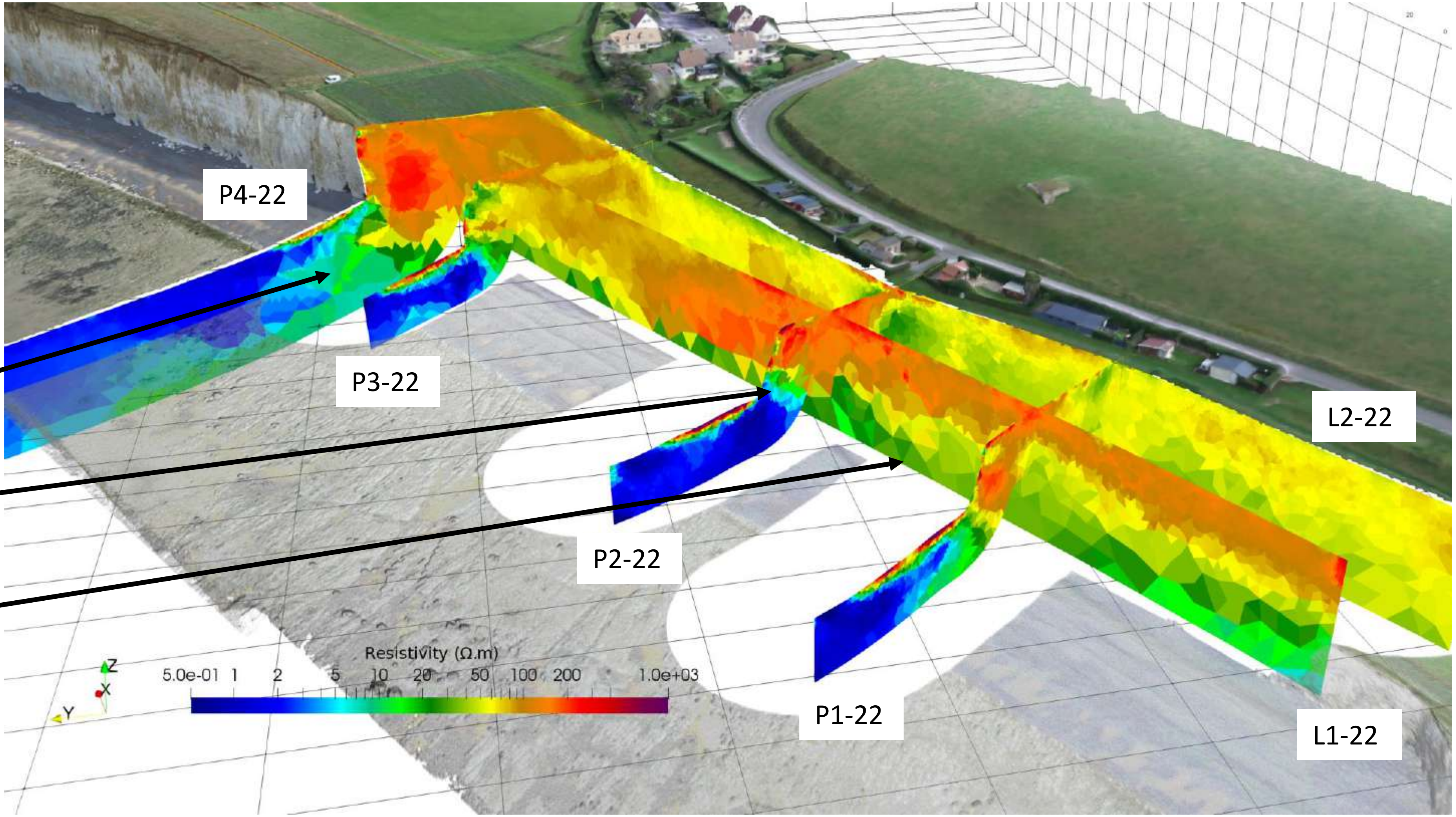

Digital Elevation Model and 3D-inverted ERT profiles : Interpretation

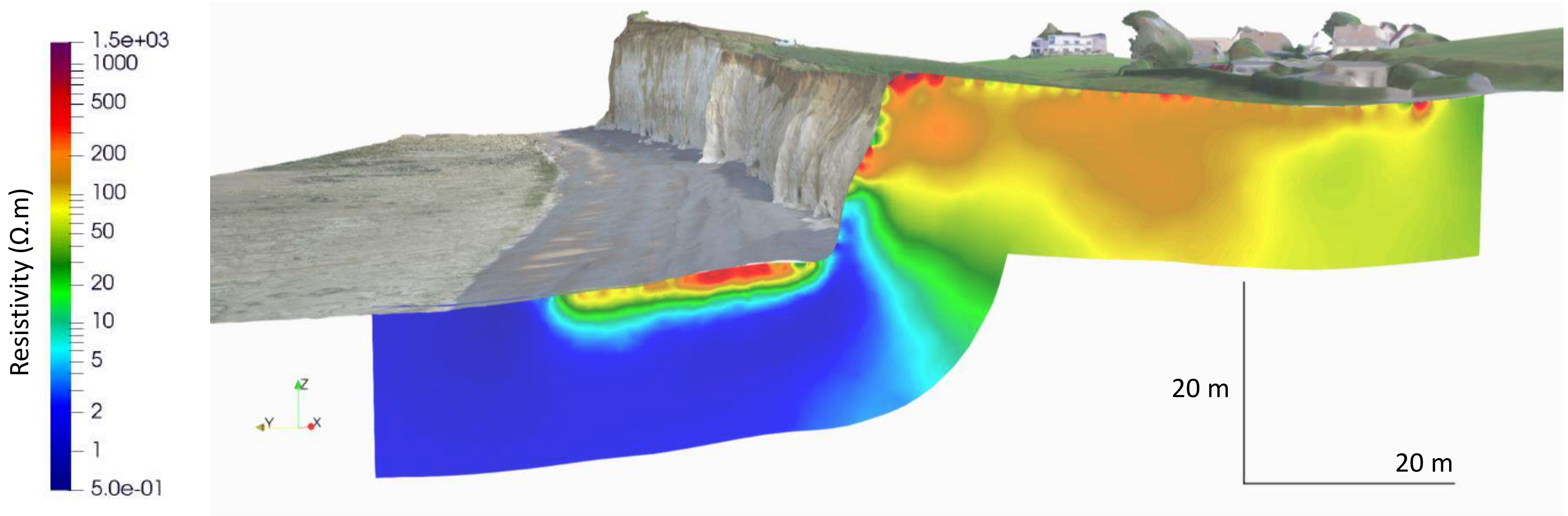

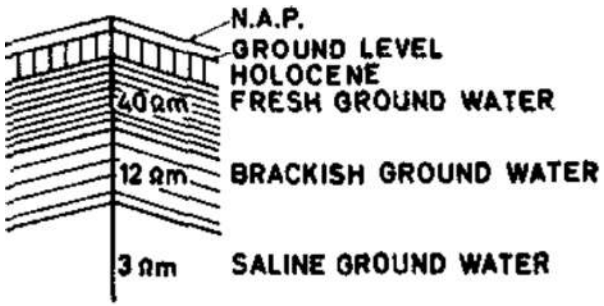

Van Dam & Meulenkamp (1967)

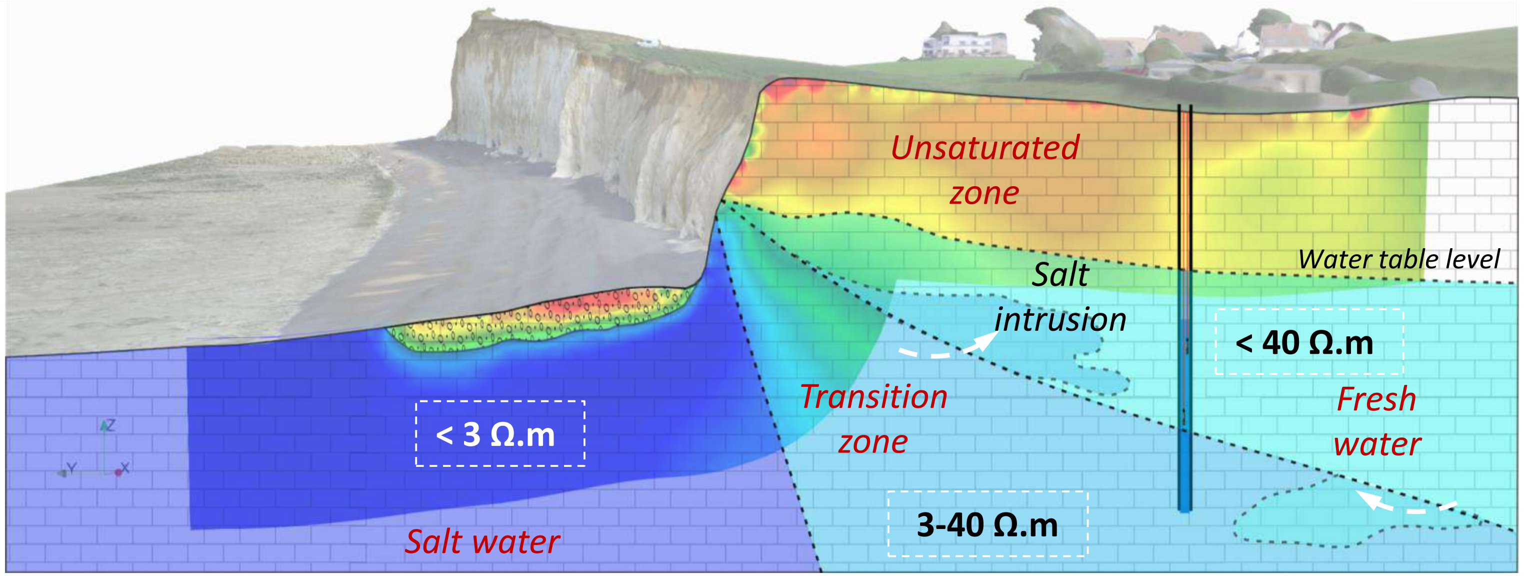

The presence of uprising brachish water

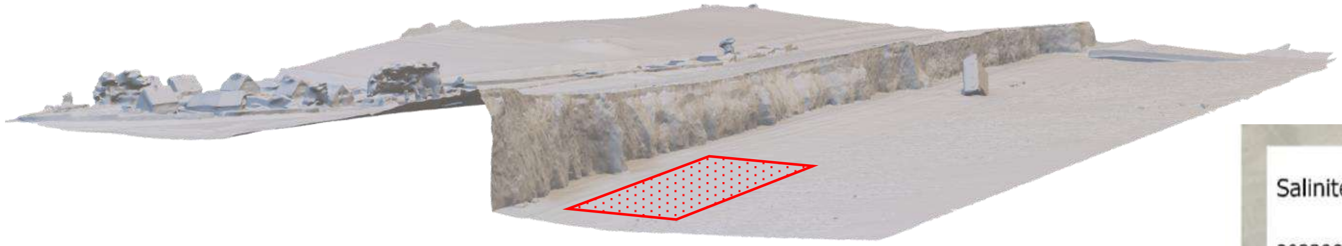

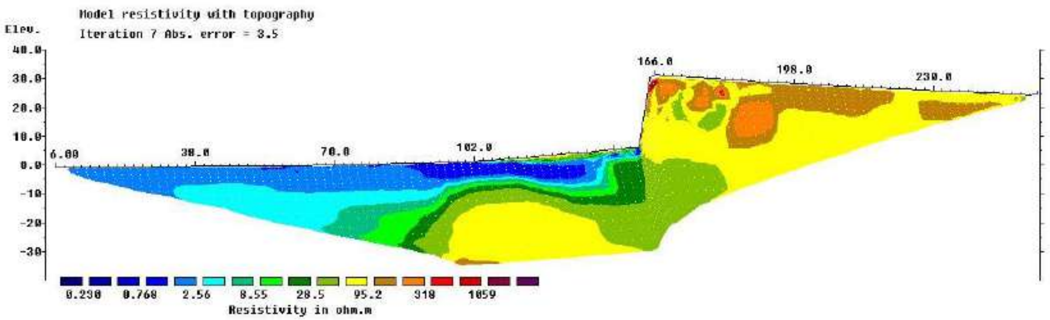

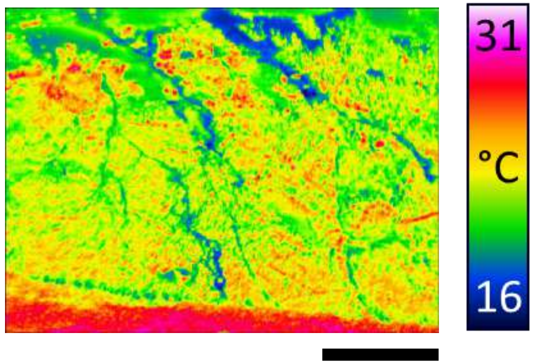

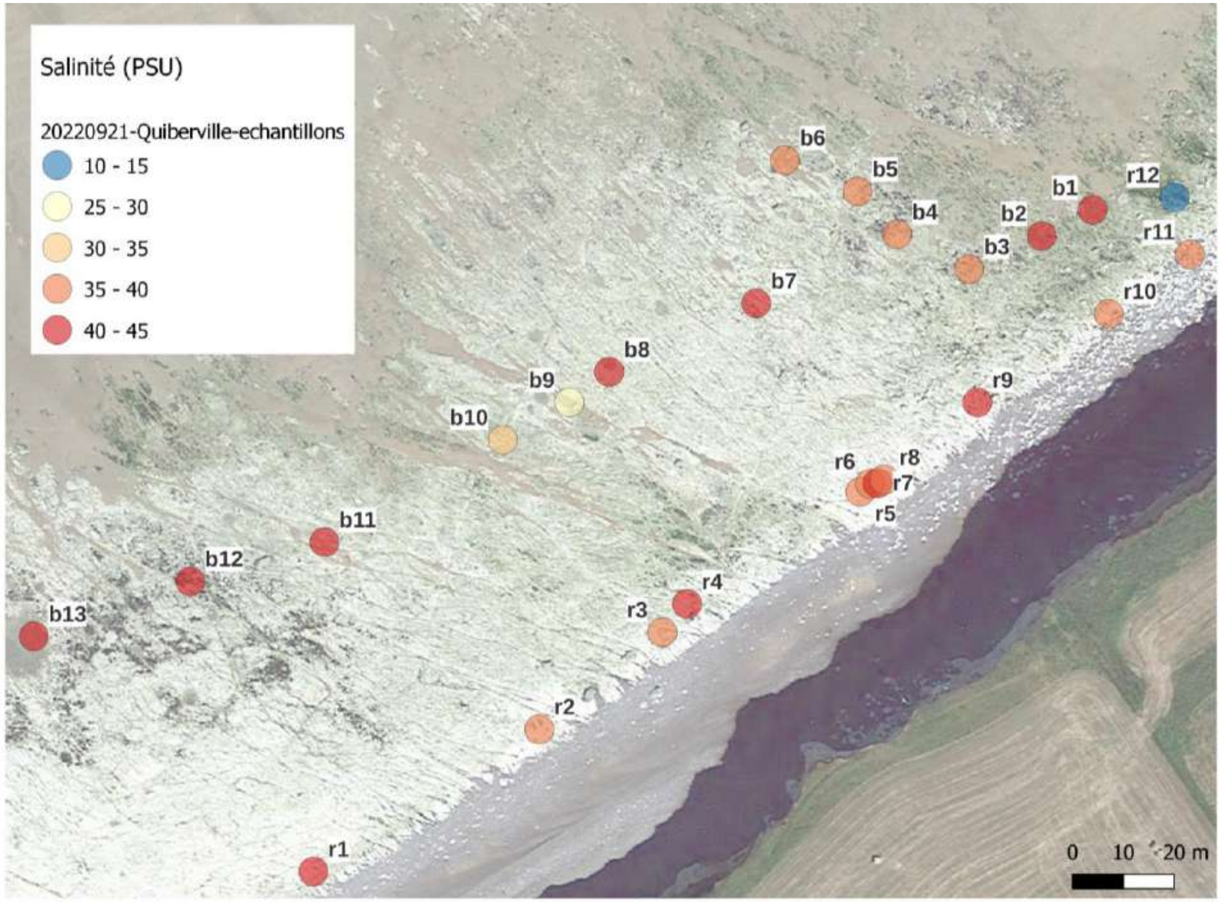

Digital Elevation Model and 3D-inverted ERT profiles

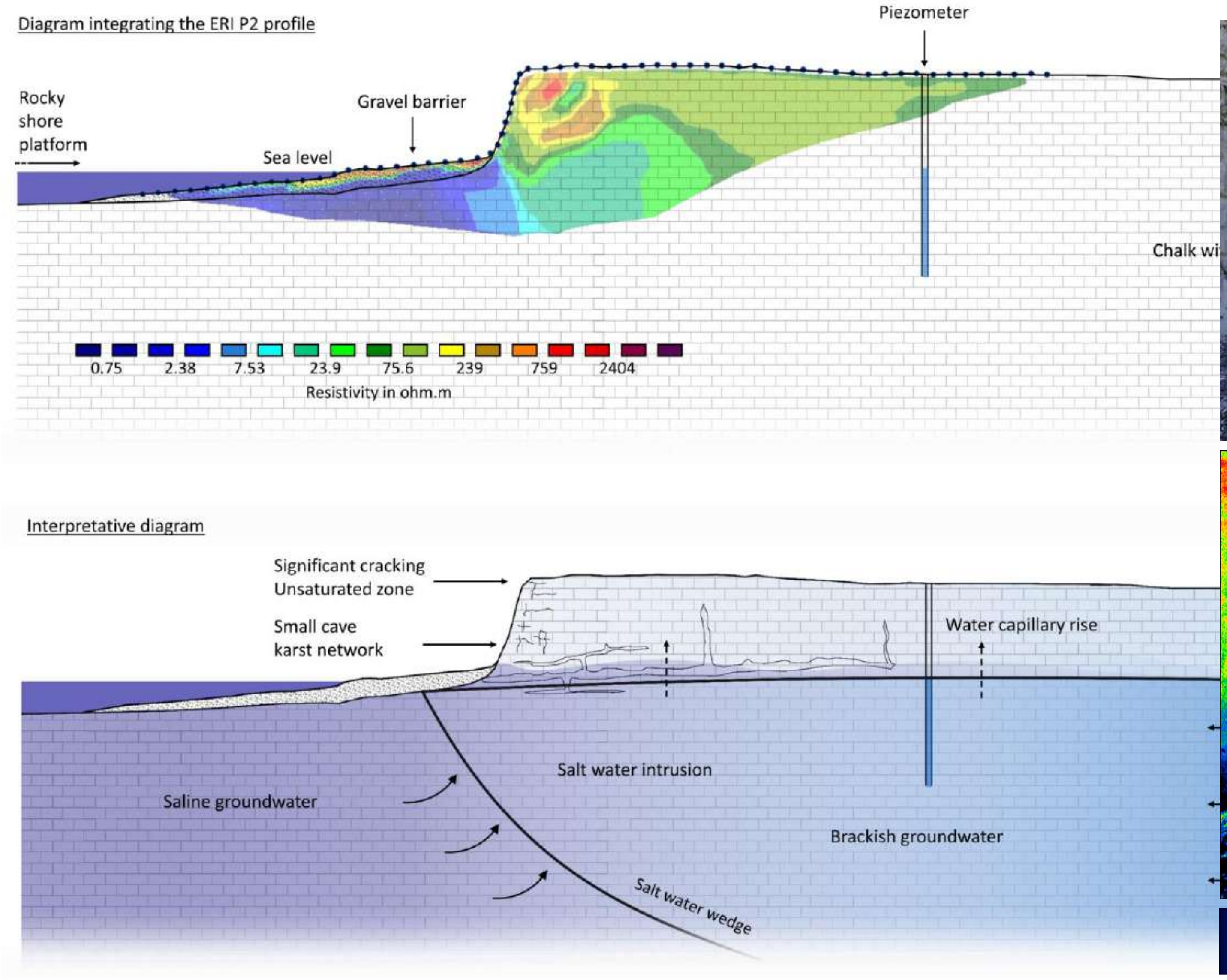

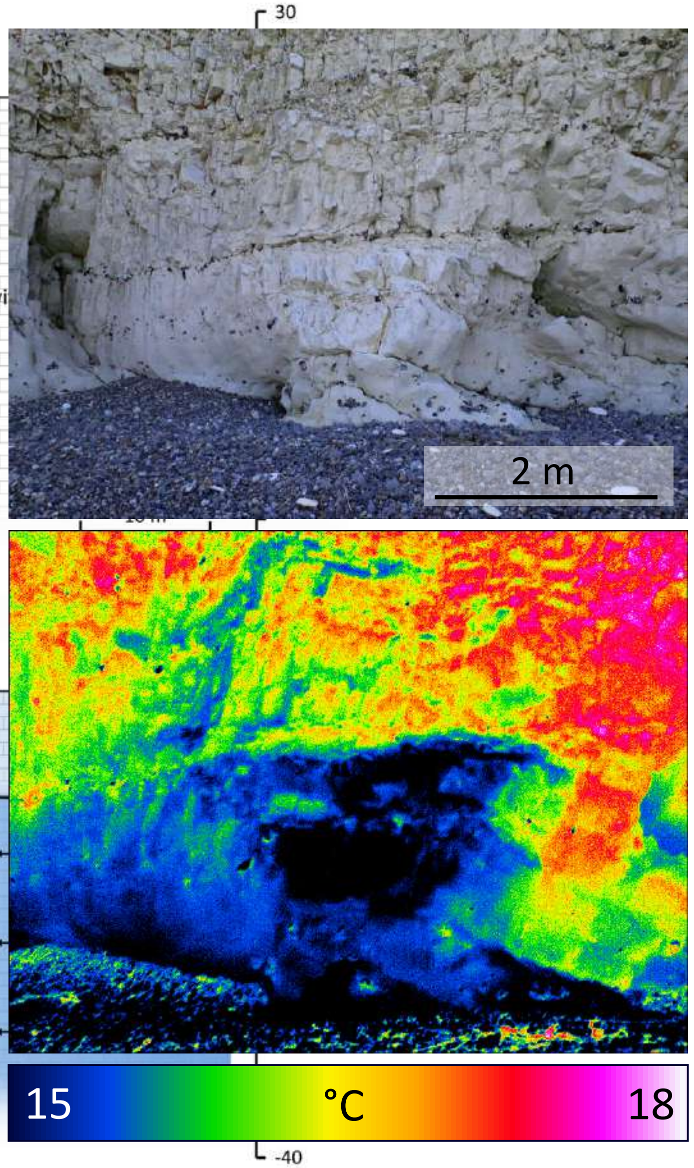

Water capillary rise as observed using temperature data

Digital Elevation Model and tTEM results

Global view with DEM and tTEM results

- All measurements DGNSS located, 1 pt/5m-10m
- Deeper DOI (~70m) than ERT
- Fast acquisition

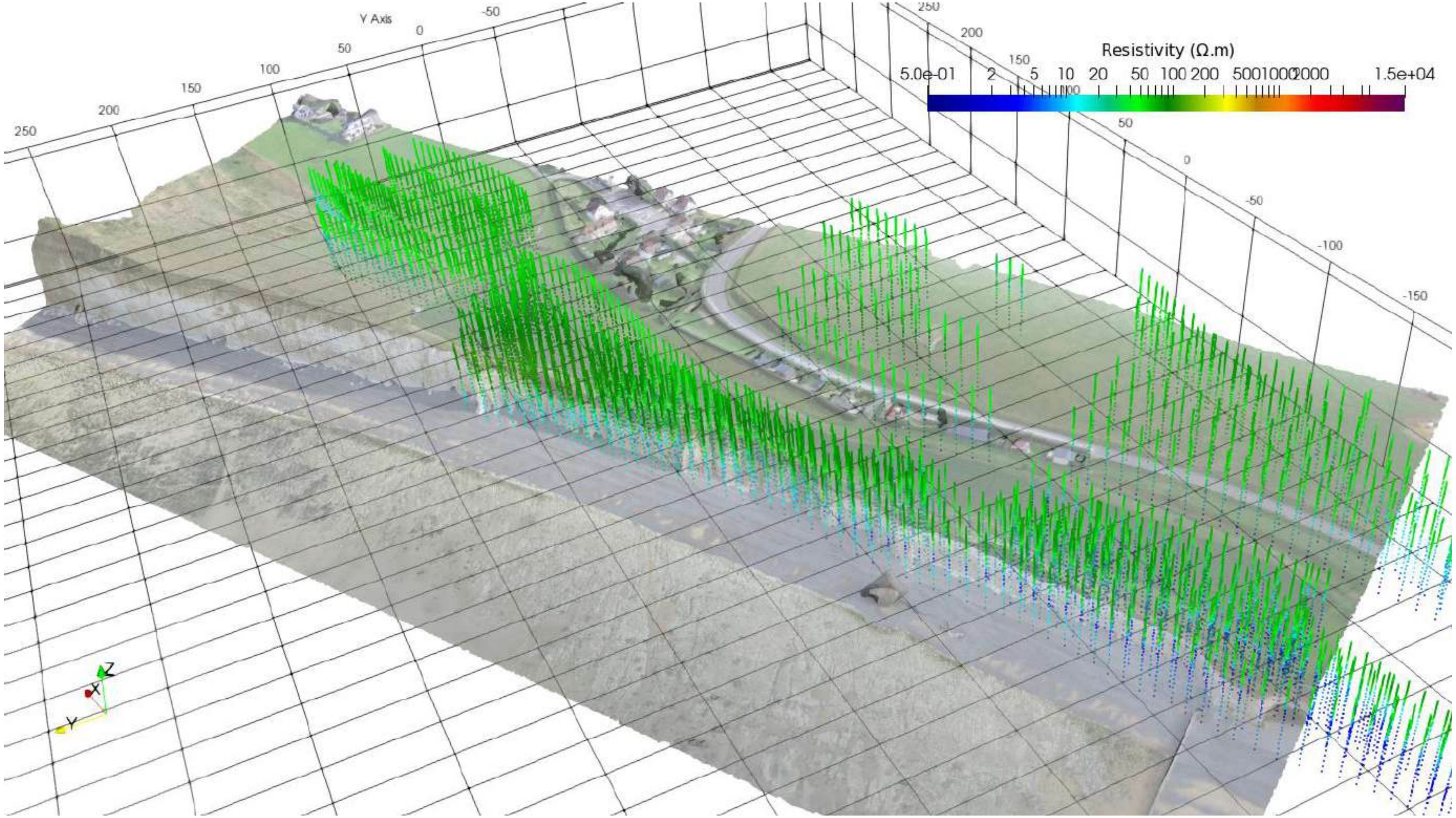

Auken et al., Geophysics, 2019

Digital Elevation Model and tTEM results

Global view with DEM (Lidar ?) and tTEM results

- All measurements DGNSS located, 1 pt/5m-10m,
- Deeper DOI (~50 to 80 m) than ERT;
- Fast acquisition

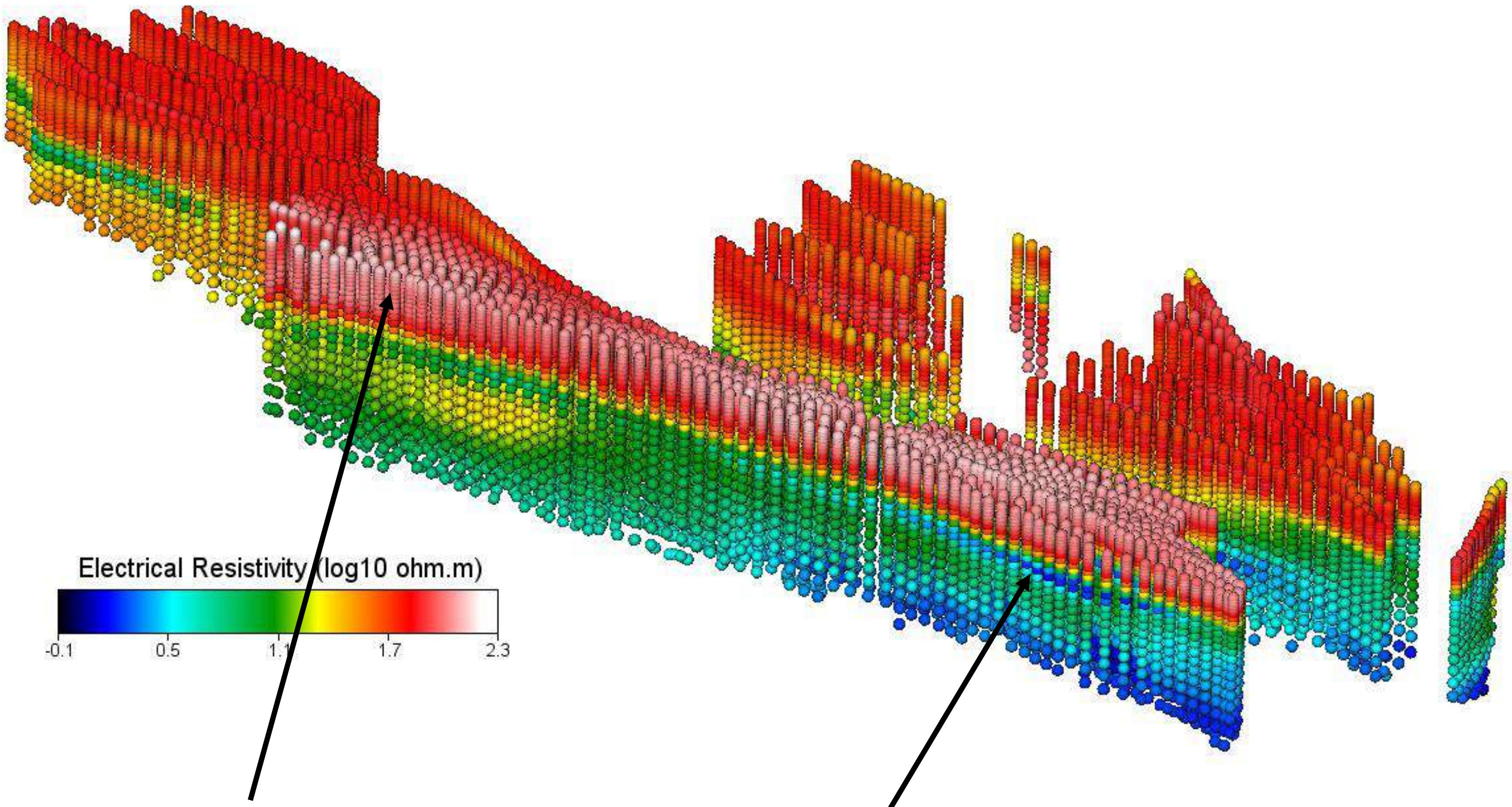

Unsaturated chalk

Very conductive anomaly: saline intrusion

Heterogeneous saline intrusion within the cliff

tTEM maps – View from the top

Interpolation between tTEM points and slices extracted at 3 elevations.

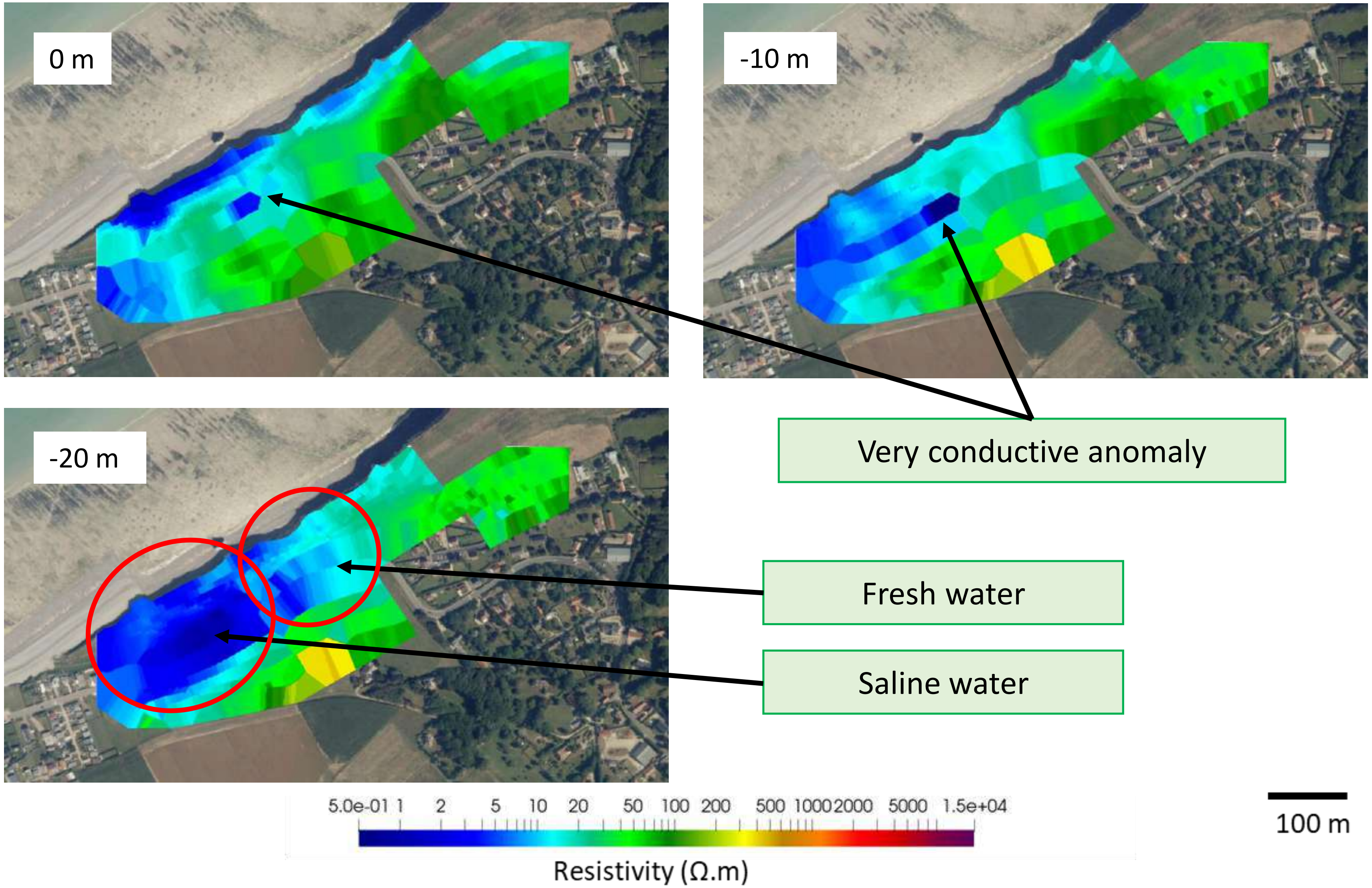

Synthesis

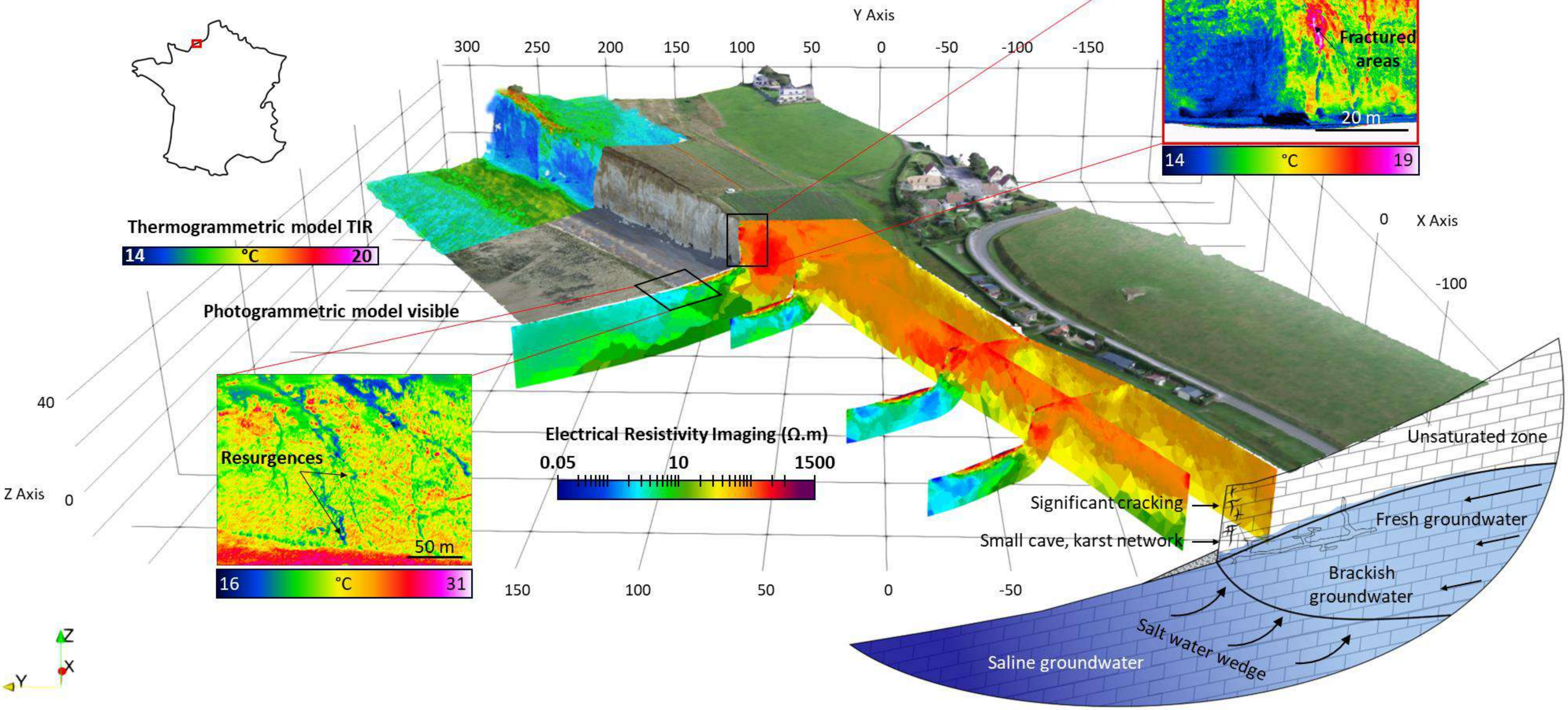
Y Axis
300
250
200
150
100
50
0
-50
-100
-150
Fractured
areas
20 m
14
°C
19
0
X Axis
-100
Thermogrammetric model TIR
14
°C
20
Photogrammetric model visible
40
Z Axis
0
Resurgences
50 m
16
°C
31
Electrical Resistivity Imaging (Ω.m)
0.05
10
1500
150
100
50
0
-50
Unsaturated zone
Significant cracking
Small cave, karst network
Fresh groundwater
Brackish
groundwater
Salt water wedge
Saline groundwater
Z
X
Y

Piezometer: presence of salt water / level variation

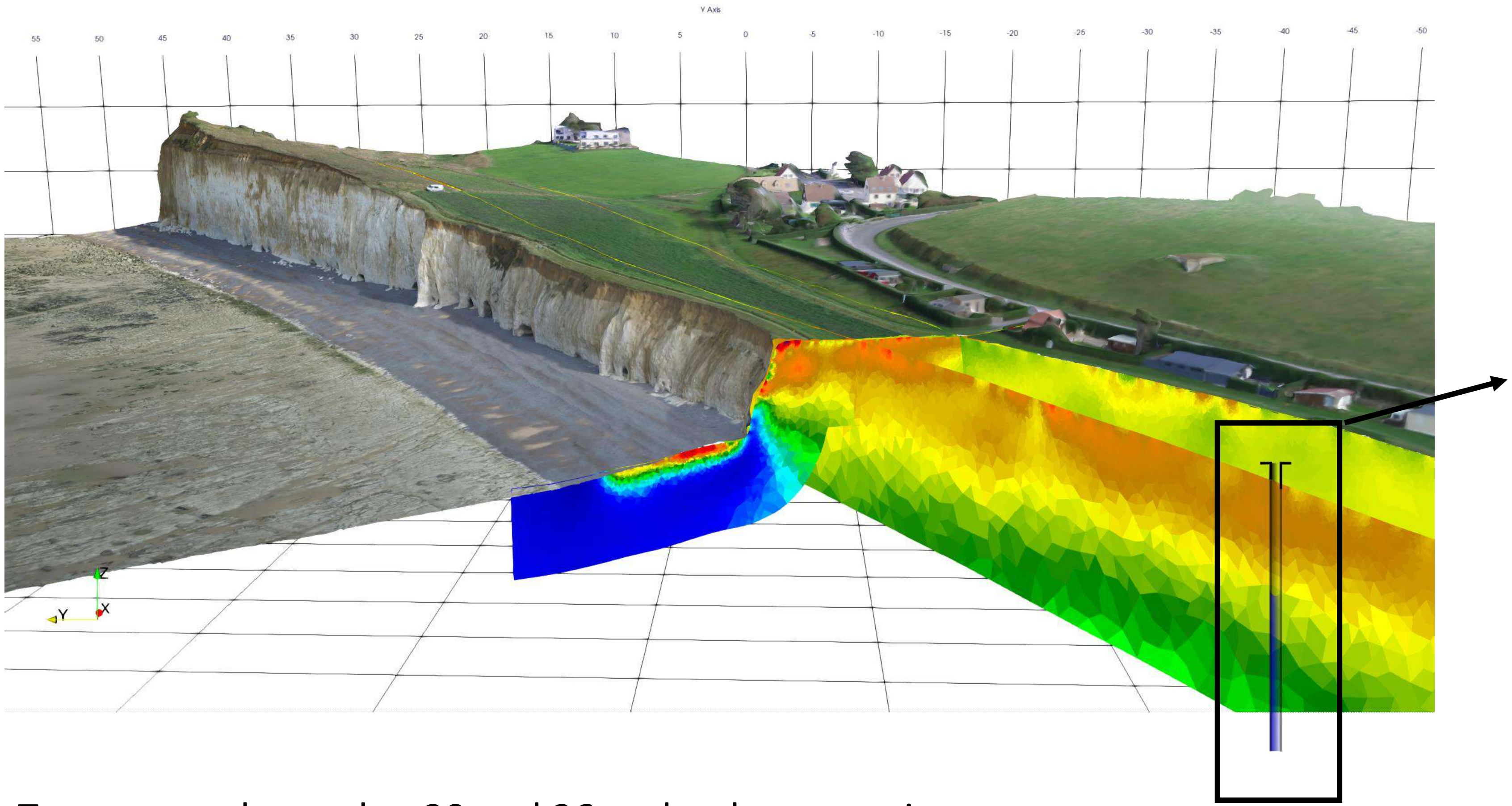

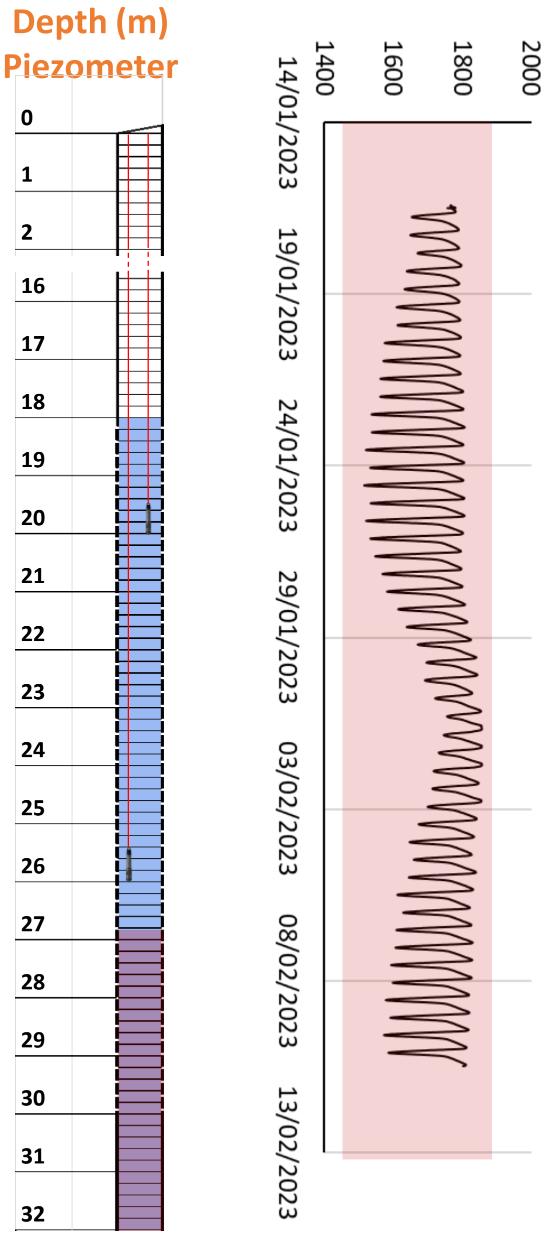

Two sensors located at 20 and 26 m depth, measuring salinity, temperature and water level located 100 m from the coast

Letortu et al., Geomorphology, 2022 and ANR Ricochet outcomes + Defhy3geo

Piezometer: presence of salt water / level variation

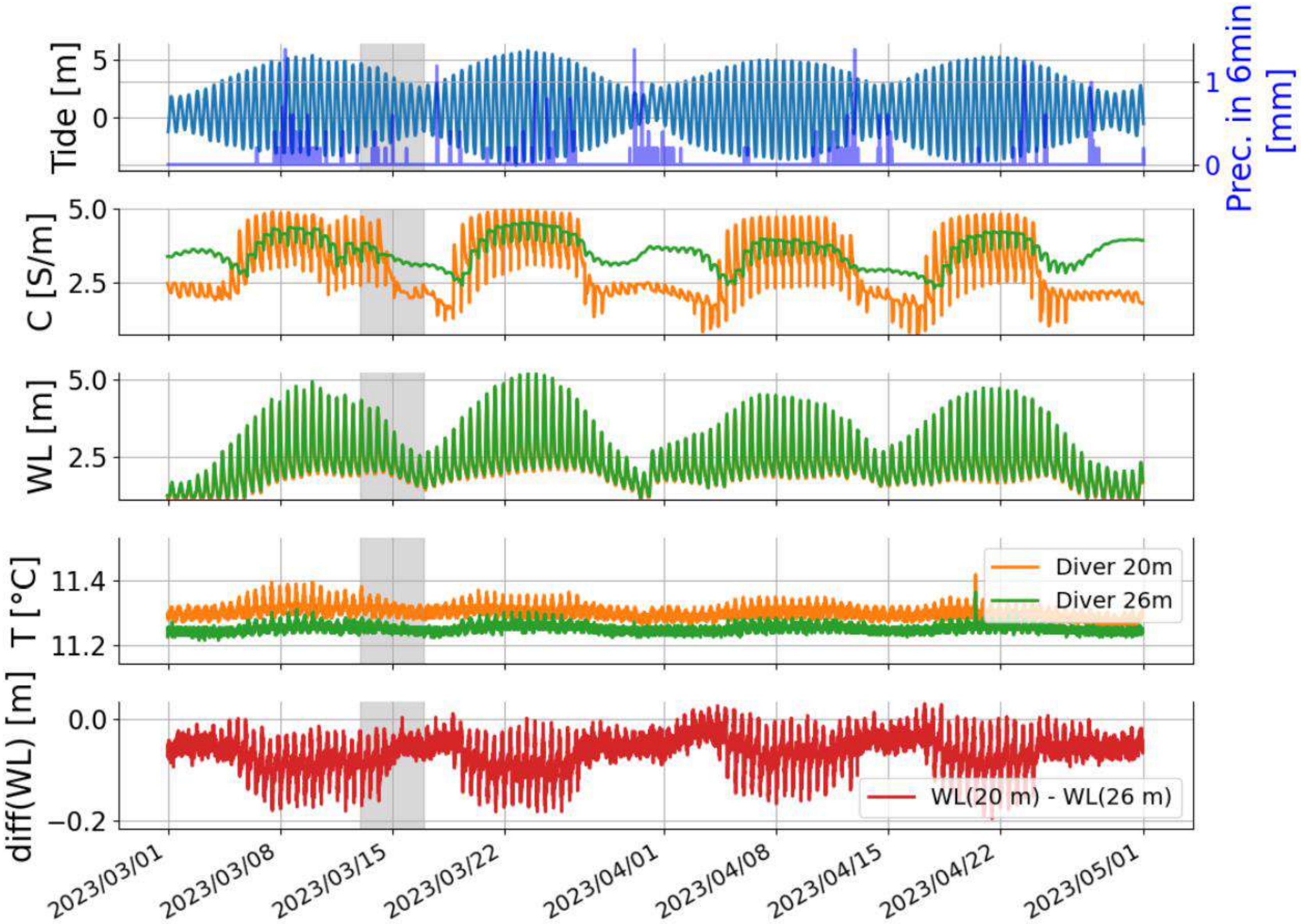

Piezometer: presence of salt water / level variation

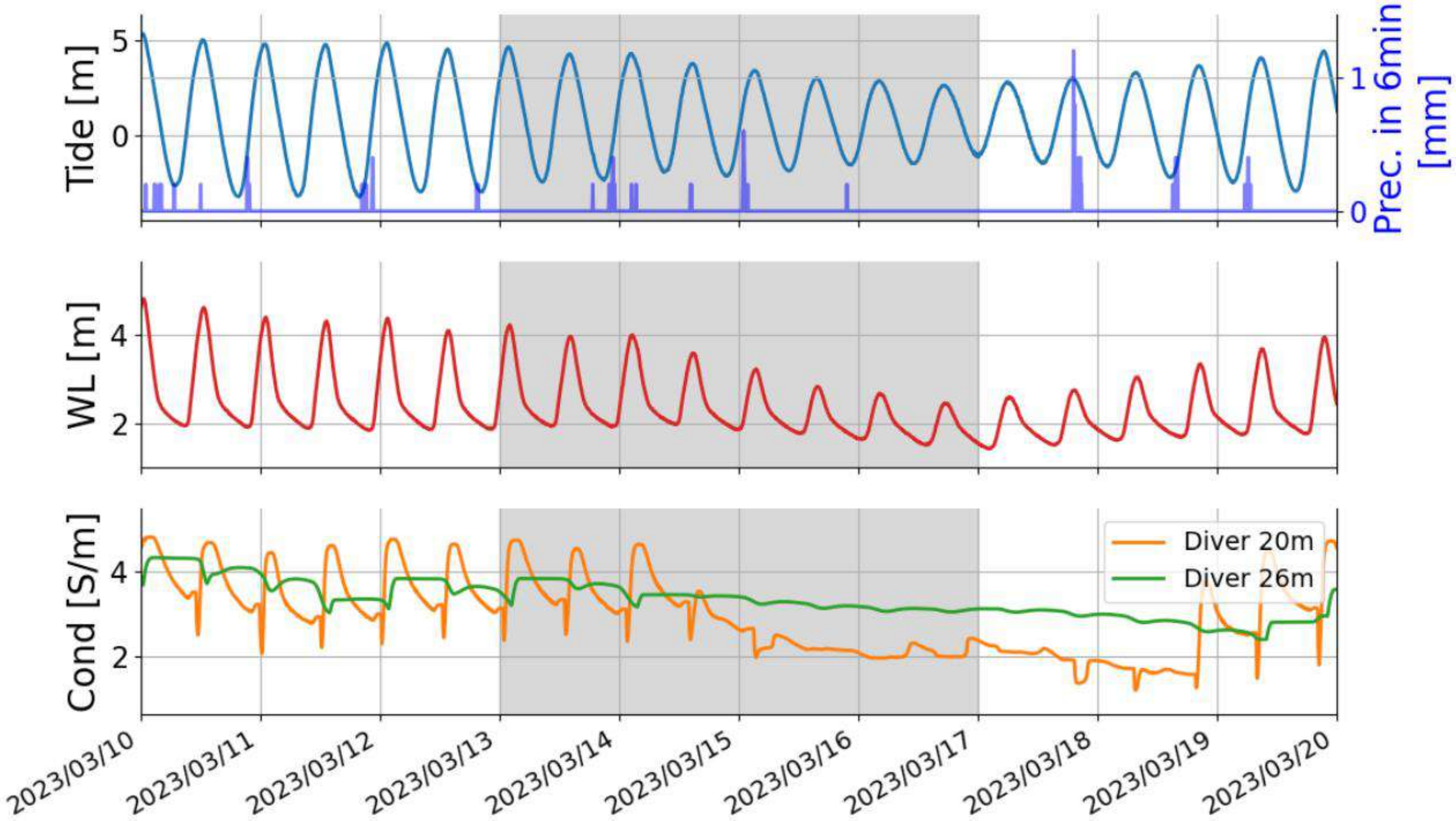

Piezometer: presence of salt water / level variation

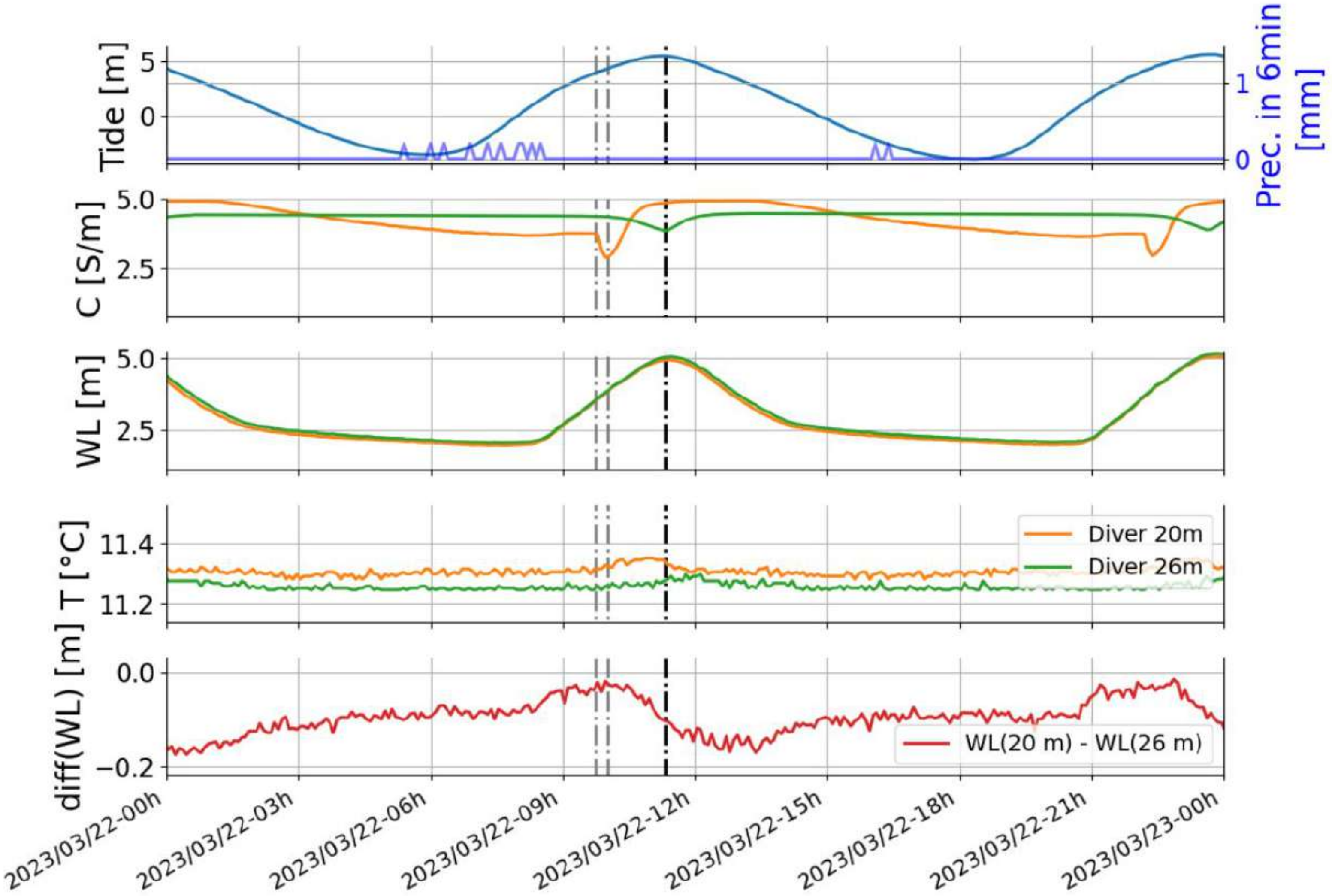

What are the physics of such signals ?

Piezometer: presence of salt water / level variation

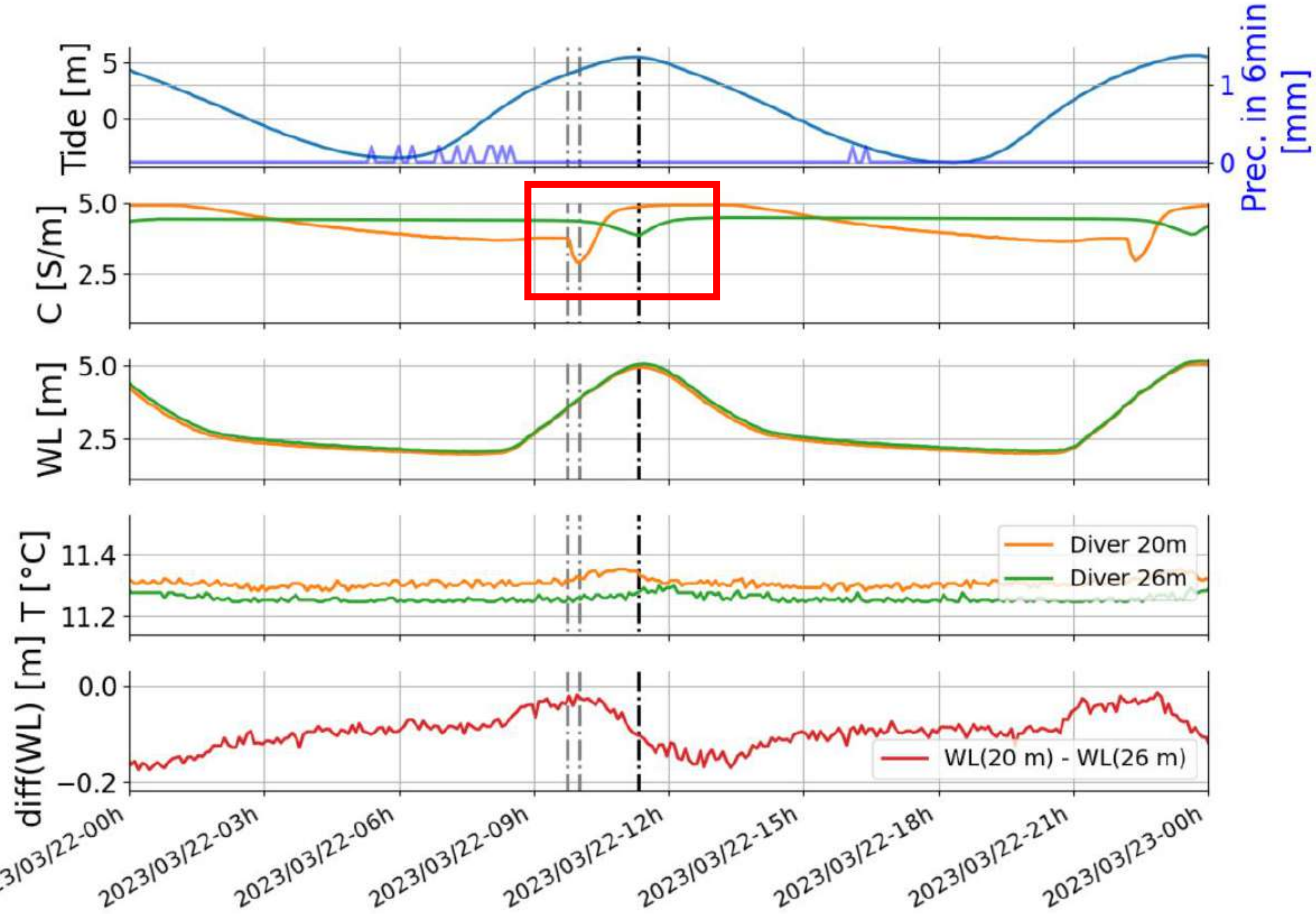

What are the physics of such signals ?

Interpretation of the piezometric data : Impact of density-driven fluctuations of salinity due to salt intrusion
Dimensionless equations for flow and solute transport

$$\frac{\partial}{\partial X}\left(\frac{\mu^r}{\kappa_z^r}\frac{\partial \Psi}{\partial X}\right)+\frac{\partial}{\partial Z}\left(\frac{\mu^r}{\kappa_x^r}\frac{\partial \Psi}{\partial Z}\right)=Ra\frac{\partial C}{\partial X} \qquad (1)$$

with

$$Ra=\frac{H\Delta\rho g\kappa_0}{\mu_0 D}, \qquad (2)$$

$$(U,W)^T=\left(\frac{\partial \Psi}{\partial Z},-\frac{\partial \Psi}{\partial X}\right)^T, \qquad (3)$$

$$C=\frac{c-c_{\min}}{c_{\max}-c_{\min}}, \qquad (4)$$

$$\phi R\frac{\partial C}{\partial T}=\frac{\partial}{\partial X}\left(\phi\frac{\partial C}{\partial X}\right)+\frac{\partial}{\partial Z}\left(\phi\frac{\partial C}{\partial Z}\right)-\left(U\frac{\partial C}{\partial X}+W\frac{\partial C}{\partial Z}\right) \qquad (5)$$

Interpretation of the piezometric data : Impact of density-driven fluctuations of salinity due to salt intrusion

a)

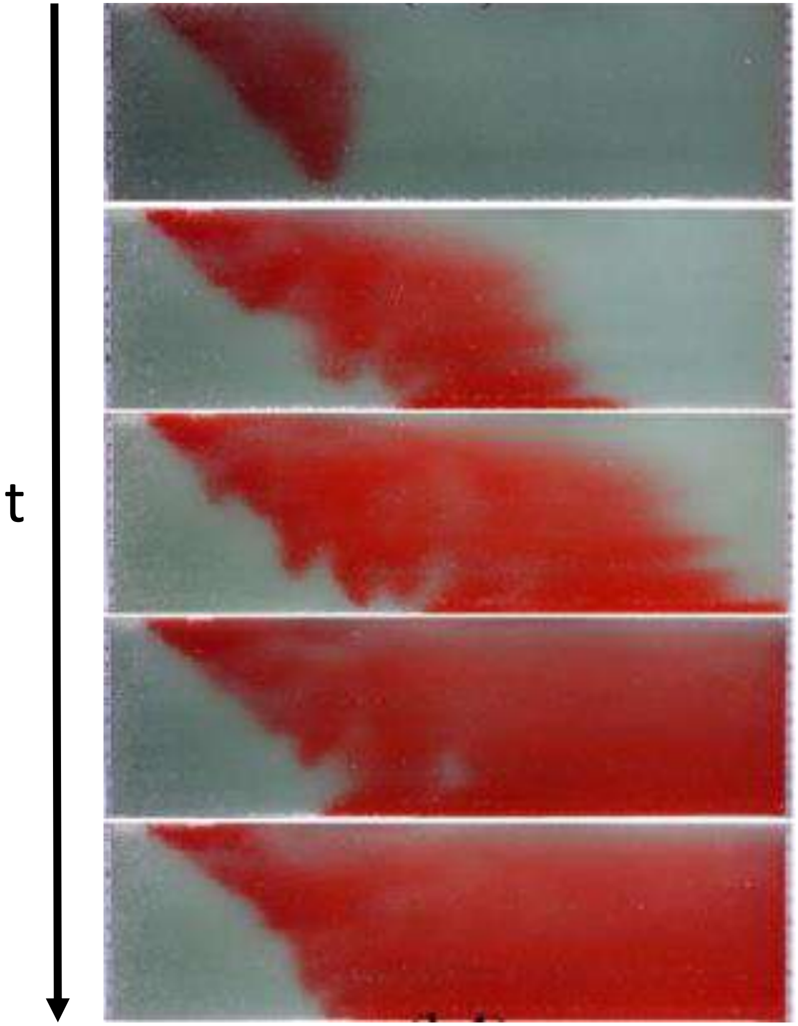

Analog experiment (Ra=162.5)
Seng et al., 2020

b)

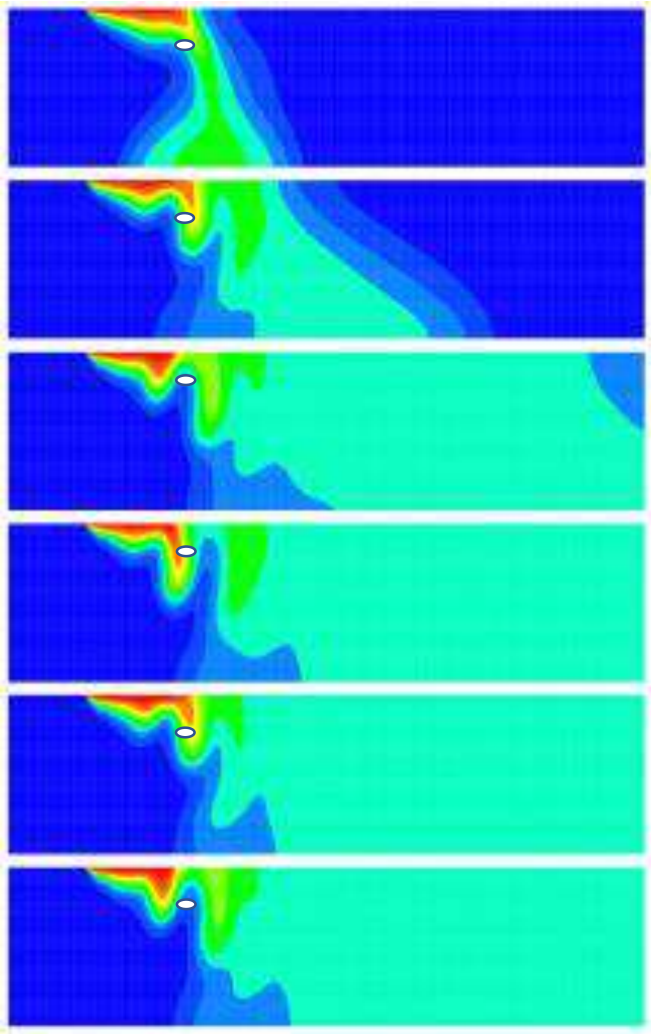

Numerical simulation (Ra=100)
Kawabata et al., 2015

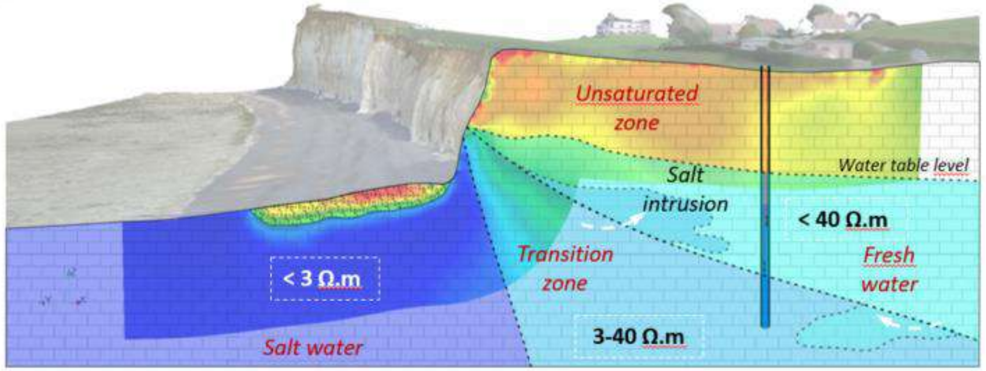

Interpretation of the piezometric data : Impact of density-driven fluctuations of salinity due to salt intrusion

b)

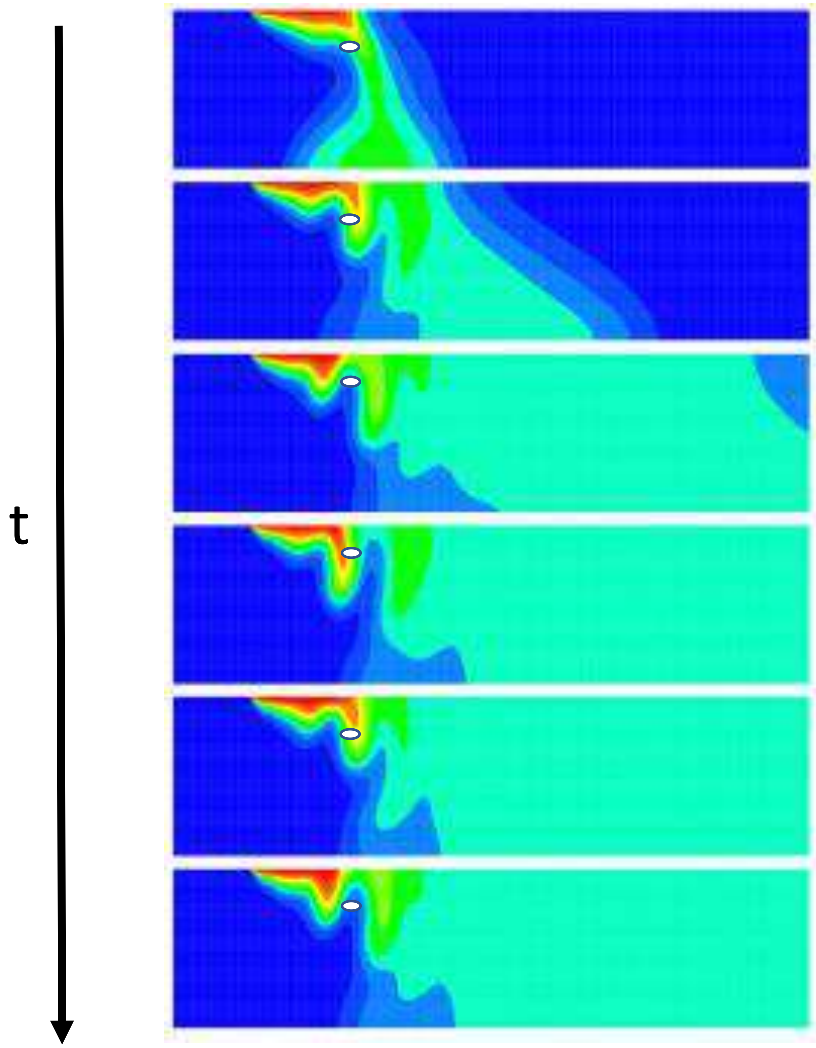

Numerical simulation (Ra=100)
Kawabata et al., 2015

Numerical results for dimensionless salinity evolution

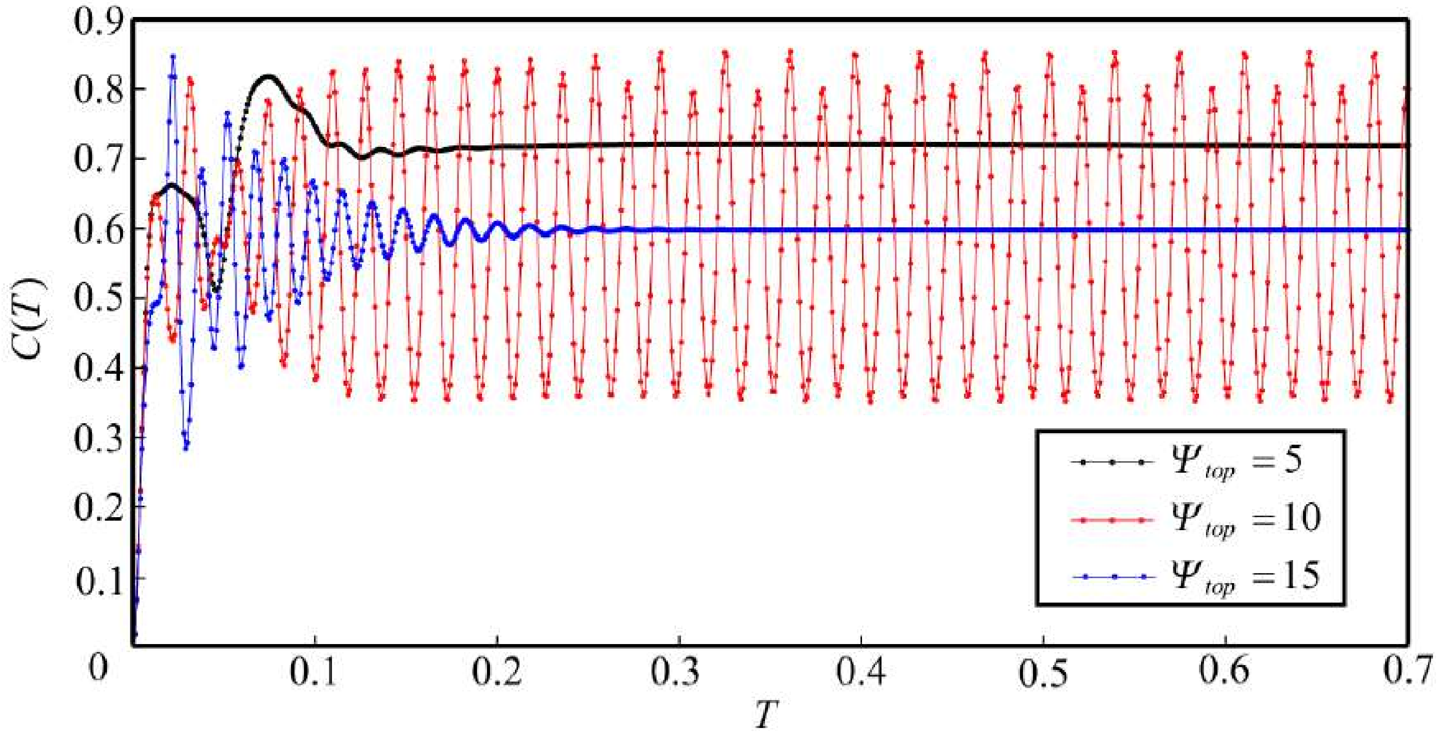

(1) rapid convergence without oscillation,
(2) oscillation, and
(3) oscillatory convergence.

Impact of density-driven fluctuations of salinity due to salt intrusion

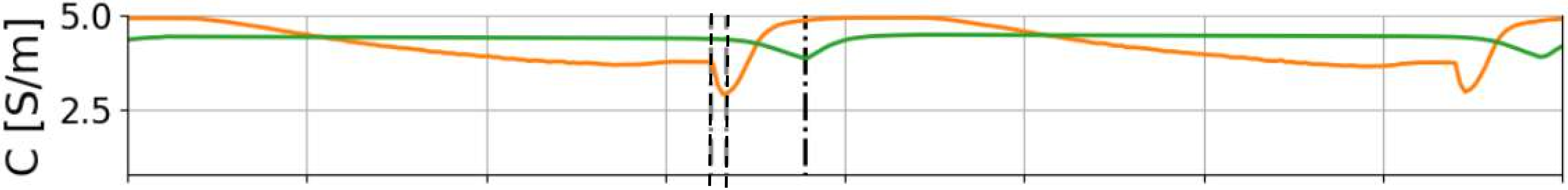

Our study

(1) rapid convergence without oscillation : not yet described in field observations !!!

>> this signal suggest a quite low Rayleigh number (~100) in the porous medium composing the cliff

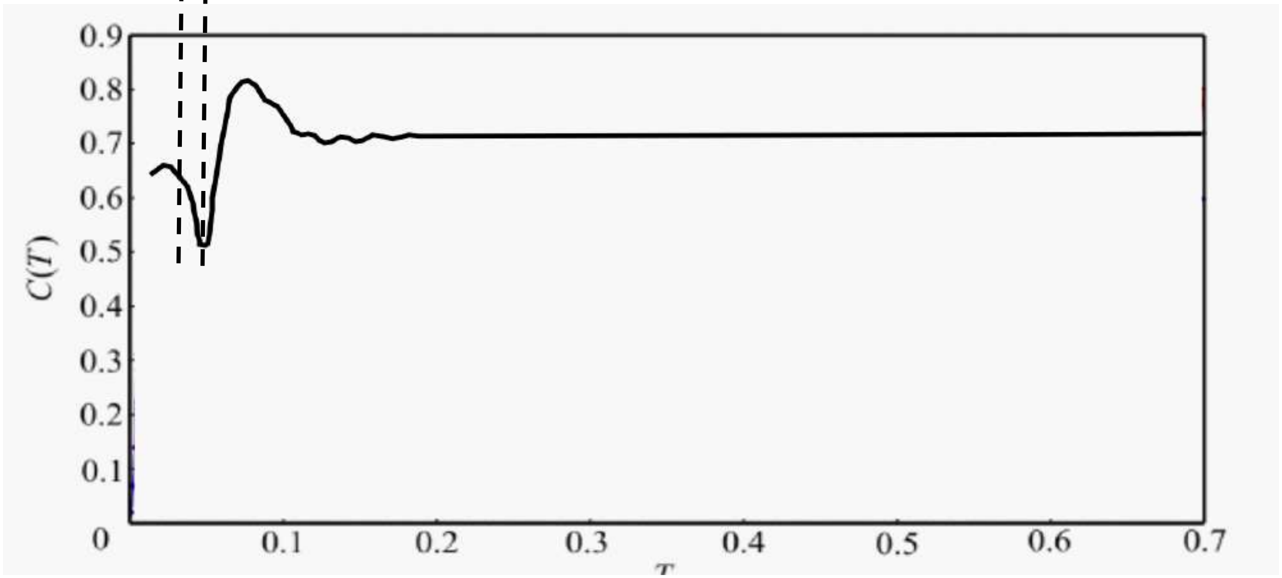

Kawabata et al., 2015

Conclusion

- We conducted crazy electric experiments on chalk cliffs in Normandy
- We produced 3D reconstitutions of the cliffs using a compilation of drone-based photography
- We built a tool to produce a reliable image of the electrical resistivity distribution within the cliff
- A saline intrusion has been mapped below the cliffs and its interaction with freshwater documented
- The freshwater seems to be impacted by density-driven saltwater intrusion, as observed in well data

What are the links between the saline intrusion
And the mechanical behavior of the cliff ?

Thank You For Your Attention

Projet Région DEFHY3GEO

Détection et Étude de la Fracturation par approche HYdrologique, GEOmorphodynamique, GEOlogique et GEOphysique.